1-1-2007

Synchronous generator transient behavior and protection under loss of excitation fault.

Hossein Tashakori
University of Windsor

SYNCHRONOUS GENERATOR TRANSIENT BEHAVIOR AND PROTECTION UNDER LOSS OF EXCITATION FAULT

by

Hossein Tashakori

A Thesis
Submitted to the Faculty of Graduate Studies and Research
through the Department of Electrical and Computer Engineering
in Partial Fulfillment of the Requirements for the
Degree of Master of Applied Science at the
University of Windsor

Windsor, Ontario, Canada

Your file Votre référence
ISBN: 978-0-494-35040-9
Our file Notre référence
ISBN: 978-0-494-35040-9

ABSTRACT

When synchronous generators are subjected to short-circuit or open-circuit in the excitation system, the accurate calculation of the machine transient performance depends on the load, power factor, open-circuit resistance and the saturation condition of their main flux paths. In this research work, computer model for synchronous generators have been developed using the IEEE3.3 equivalent circuit utilizing flux and current differential equations. Main flux saturation and governor control loop were considered in the developed model. The generator terminal impedance, seen by an impedance relay, takes a certain period of time to fall to the relay characteristic circle. The effect of the main flux saturation both in the direct and quadrature axes on the determination of the transient performance and seen impedance by the protective relay of synchronous generator is demonstrated in this research work.

DEDICATION

This thesis is dedicated to my wife and my lovely daughter who offered me unconditional support throughout the course of this thesis. They stood beside me when I facing all difficulties. Also I would like to give special respect to my father spirit that his lost during this work had a large impact on my life. GOD BLESSES HIM.

ACKNOWLEDGEMENTS

I wish to take the opportunity to thank my supervisor Dr. N. Kar for his technical guidance, supportive advice and his understanding to some of the difficulties I went through. Thank you for your inspiration at times when I was feeling blue. Sincere thanks to my examination committee members Dr. K. Tepe and Dr. S. Das for taking the time to review my work. I would like to also thank my fellow graduate students for their helpful criticism and suggestions.

TABLE OF CONTENTS

LIST OF TABLES

LIST OF FIGURES

LIST OF SYMBOLS

V_t	:Terminal voltage
I_t	:Terminal current
P_t	:Terminal real power
V_d, V_q	:d- and q-axis components of the stator voltage
V_{kd1}, V_{kq1}	:d- and q-axis rotor damper winding voltages
E_{pm}	:Equivalent permanent magnet voltage
i_d, i_q	:d- and q-axis components of the stator current
i_{kd1}, i_{kq1}	:d- and q-axis rotor damper winding currents
i_{md}, i_{mq}	:d- and q-axis components of the magnetizing current
i_{pm}	:Equivalent permanent magnet current
ψ_d, ψ_q	:d- and q-axis components of the stator flux linkage
ψ_{kd1}, ψ_{kq1}	:d- and q-axis damper winding flux linkages
ψ_{pm}	:Permanent magnet flux
ψ_{md}, ψ_{mq}	:d- and q-axis components of the magnetizing flux linkage
AT_d, AT_q	:d- and q-axis amperes-turns
R	:Stator winding resistance
R_{kd1}, R_{kq1}	:d- and q-axis rotor damper winding resistances
X_d, X_q	:d- and q-axis synchronous reactances
X_{kd1}, X_{kq1}	:d- and q-axis damper winding reactances
X_{mds}, X_{mqs}	:d- and q-axis saturated magnetizing reactances
X_{mdu}, X_{mqu}	:d- and q-axis unsaturated magnetizing reactances
X_l	:Stator leakage reactance

T_e	:Electromagnetic air-gap torque
ω_s	:Synchronous speed in rad/sec
ω_r	:Rotor mechanical speed
H	:Moment of inertia of the rotor
PF	:Power factor
δ	:Load angle
θ	:Power factor angle
V_B	:Infinite bus voltage
t	:Time
Δt	:Time step
n	:Time counter
t_n, t_{n+1}	:Present and next time step

1. Introduction

1.1 Synchronous Generator Protection Review

Synchronous generators supply almost all the electric power we consume today. The rotor of a synchronous generator needs to be driven by a source of mechanical power or prime mover and the field winding needs to be fed by a source of DC power in order to provide active and reactive power to the power system. These exclusive combinations of electrical and mechanical equipment need to be protected against different kinds of faults. Generator faults are always considered to be serious since they can cause severe and costly damage to insulation, windings, core, shafts and couplings [1]. Protective relays using variety of signals are meant to monitor and provide proper signals to alarm or remove the generator from the system under faulty conditions. Such abnormal conditions and associated protective devices will be discussed in the next section. AMERICAN NATIONAL STANDARD INSTITUTE [ANSI] numbers of the protective devices are listed in [2].

1.1.1 Synchronous Generator Protection Relays

Abnormal conditions of a generator could be in the stator or in the rotor field [3]. Figure1 illustrates a typical generator protective scheme. Each protective device could be a stand alone relay or multi function relay. With the introduction of fast CPUs, numerical relays contain more than one protective device are very common. Use of multi function relays has advantages of simplicity in testing and calibrating, saving panel space, faster and easier installation and wiring [4]. As Figure 1 [5] shows the relay needs different analog signals representing generator working conditions such as voltages, currents, and temperature. These signals are being provided to the relay by sensors and current and voltage transformers. Numeric relays using digital processing techniques converts these analog signals to a discrete signal and with different algorithm the amplitude and phasor angle of the signal could be obtained. The numeric procedures are explained in [6]-[9]. With these signals, relay will internally calculate the other parameters needed for a particular protective function. If calculated parameter exceeds the relay settings set for the particular generator, the relay will provide the appropriate signal for tripping or alarming purposes.

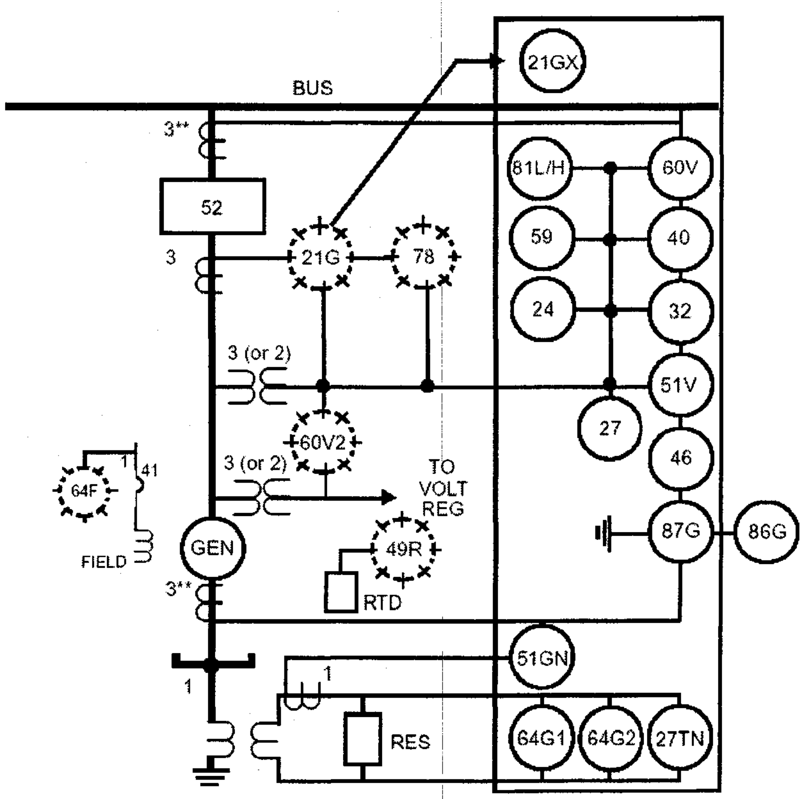

Fig. 1. Generator protection scheme [5].

1.1.2 Brief Description of the Synchronous Generator Protective Devices

Each protective function represented by an ANSI number [2] is well known in industry. In this section the devices shown in Figure 1 will be briefly explained in numerical order.

Device 21: Distance relay

This relay is an impedance relay which uses voltage and current phasors to measure the impedance in front of the generator. Basically this device protects the generator from an external fault. If this impedance falls into the relay characteristic, relay will trip the generator. Figure 2 illustrates a typical distance relay characteristic and the impedance trace after fault [10].

Device 24: Overexcitation relay

This relay uses voltage and frequency to calculate the ratio V/Hz and if the value exceeds 1.05 per unit (pu), the relay picks up. Overexcitation can occur during start-up or shutdown at reduced frequency. This abnormal condition can cause localized hot spot in the stator, lamination damage and field over-temperature [3],[11].

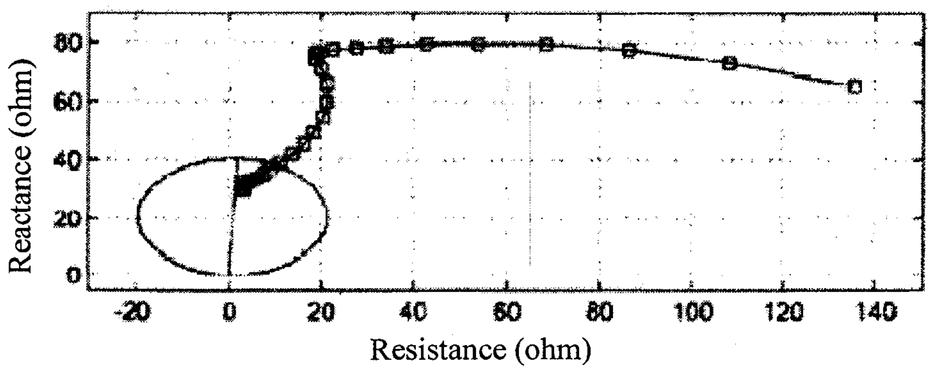

Fig. 2. Typical distance relay characteristic [10].

Device 27: Under-voltage relay

This device monitors the generator voltage and will provide signal if the voltage drops under the limit. Voltage measurements can be used to detect that something unusual is happening on the system, but generally this information will not give any indication of the location of the problem. Hence, measurement of voltage is usually reserved for overall system protection functions [12].

Device 32: Power direction relay

This device is a reverse power relay which monitors the direction of generator power to prevent any reverse flow of active power (motoring mode of operation). Motoring is an abnormal condition that can cause serious mechanical damage to prime mover. A time delay is always associated with this device to let normal power swing and synchronizing. In some applications this relay could be used for load shedding [13].

Device 40: Loss of Excitation

This device is an impedance relay connected to generator terminals to monitor generator impedance. When a generator loses excitation, it operates as an induction generator running above synchronous speed [14]. Under such condition the generator impedance enters the relay characteristic. This relay will be discussed in detail in this research work.

Device 46: Current unbalance

This device monitors the negative sequence component of the current and if this current exceeds from the relay setting, relay will operate. The most common causes of unbalance current are system asymmetries, unbalance loads, unbalance fault and open phase [3]. These system conditions produce negative-phase-sequence components of current which induce a double-frequency current in the surface of the rotor, the retaining rings, the slot wedges, and to a smaller degree, in the field winding. These rotor currents may cause high and possibly dangerous temperatures in a very short time [13].

Device 49: Over temperature

This device senses the temperature through RTD or TC at different spots of the generator and provides a thermal protection. Usually this relay is not used for primary protection [5].

Device 51: Time delay over current

This device monitors currents flowing through generator windings and provide a time delay over load protection for the particular part. The relay has an inverse time characteristic and provides a time delay which is inversely proportional to the over load current magnitude [15]. Device 51V is the voltage restrained time delay over current relay which provides better protection when under voltage condition exists [13].

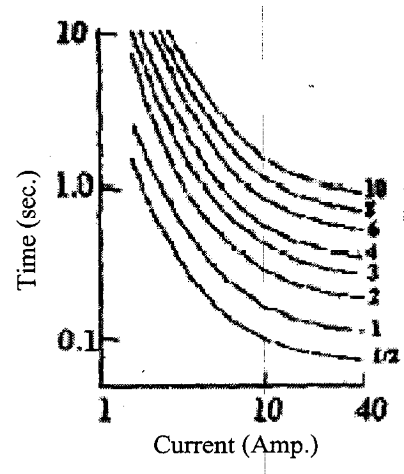

Fig. 3. Typical over current relay characteristic [15].

Device 59: Over voltage relay

Over voltage relay is for monitoring the voltage and if the voltage exceeds from the relay preset level, it will trip. Over-voltage can shorten insulation life and accelerate insulation failure.

Device 60: Voltage Balance

This device compares two voltages from two different set of voltage transformers (VTs) and kicks in if these two voltages are not balanced. Most common use of this relay is to detect VT fuse failure. If a fuse blows in the protective relay, the relay will alarm and block possible incorrect tripping by protective relays whose performance may be affected by the change in potential. Typical relay functions such as 21V, 40V, and 51V are normally blocked [13].

Device 64: Ground fault

The function of this device is to detect ground fault in the stator or rotor field winding. It is a common practice to ground all types of generators through some form of external impedance. The purpose of this grounding is to limit the mechanical stresses and fault damage in the generator, to limit transient voltages during faults, and to provide a means for detecting ground faults within the generator. The magnitude of stator ground-fault current decreases almost linearly as the fault location moves from the stator terminals toward the neutral of the generator [16]. For a ground fault near the neutral of a wye-connected generator, the available phase-to-ground fault current becomes small regardless of the grounding method. Therefore typical over current relays are not suitable to detect ground fault.

Device 78: Out-of-step relay

This function of this relay is to detect the loss-of-synchronism condition of the generator. The relay contains of two blinder elements supervised by a mho relay to prevent nuisance tripping for stable swings. Figure 4 illustrates the relay characteristics [17]. The basic operation of this relay is the same as LOF relay and it will well explained in the next chapter.

Device 81: Over/Under frequency

This relay is to detect abnormal frequency conditions. The operation of generators at abnormal frequencies (either over-frequency or under-frequency) generally results from full or partial load rejection or from overloading of the generator. Full or partial load rejection may be caused by clearing of system faults or by over-shedding of load during a major system disturbance. Load rejection will cause the generator to over-speed and operate at some frequency above normal [3]. Multi stage under frequency relay can be used for automatic load shedding [18].

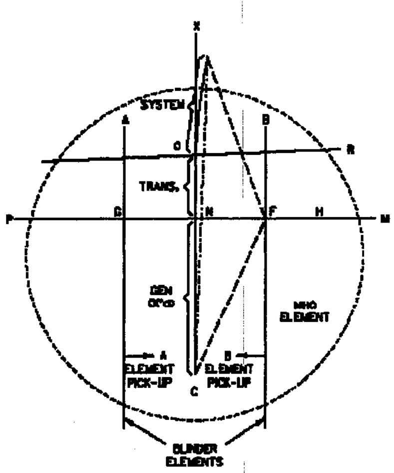

Fig. 4. Out of step relay characteristic [17].

Device 87: Differential Relay

This relay looks into a zone defined by location of current transformers and if the input current does not match with output current in that zone, it rapidly trips the generator. The most common differential relay is variable slope relay. In this relay there are two main parts or coils. One is operating part and the other is restraint part. The slope of relay characteristic varies with the values of through current. Figure 5 illustrates differential relay characteristic [19].

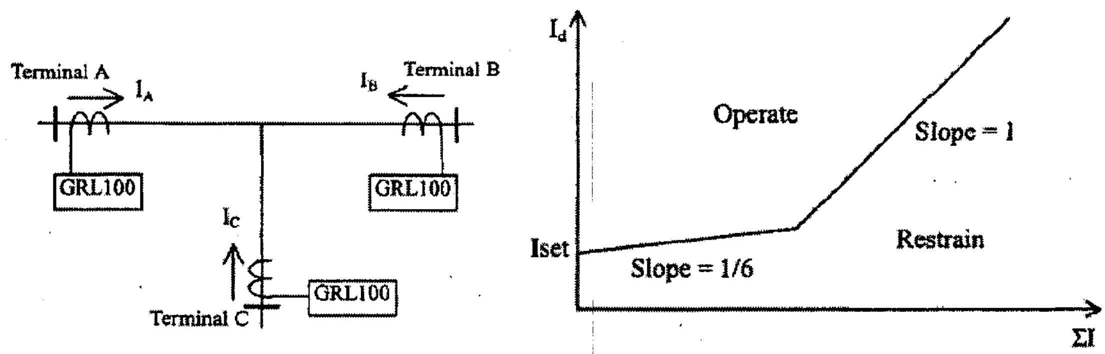

Fig. 5. Differential relay characteristic [19].

1.1.3 Loss of Field or Excitation Protection (LOF)

The field circuit of a synchronous generator needs to be excited by a direct current supply in order to keep generator in synchronism with the power grid and to keep the voltage constant. Basically synchronism between the power system and the generator is maintained due to the interaction of fluxes produced by the stator and rotor windings [20]. Excitation can be provided in many ways including rotating dc exciters with commutators, rotating alternator rectifier or static supplies. Power and torque pulsation due to LOF conditions will be more severe on a generator with rectifier bridge supply than for generator supplied by dc exciter [21]. After LOF occurs, the decrease in the field current leads to a decrease in the electromagnetic torque while the mechanical torque from the prime-mover can not change immediately, thus the rotor will accelerate. Under such condition, the generator speed will be above the synchronous speed and the synchronous generator will operate as an induction generator. Due to the slip between the rotating magnetic fields of the stator and the rotor, ac currents are induced in the field winding body and damper windings [20], [22]. Because of reactive power drawn by the LOF generator the system voltage is immediately reduced while the armature current of the generator is increased [23]. Under such circumstances, disturbance in the power system would take place [24]. The most common causes of loss of excitation include [25]:

- Loss of field to the main exciter
- Accidental tripping of the field breaker
- Short circuit in the field circuit
- Poor brush contact in the exciter
- Field circuit breaker latch failure
- Loss of ac supply to the excitation system

Since the rotor of large turbo generators is not laminated, instead being machined from a steel alloy forging, under loss of excitation condition, substantial heat will be generated by eddy currents [20],[26],[27]. Excess rotor heat is likely to affect the integrity of the field windings, insulation, wedges or retaining rings [21]. Damage to the generator can occur in a timescale of between 10 second and several minutes [28], [29].

The loss of excitation can be detected by field under-current and under-voltage relay [30]-[32]. It has been reported that such relaying can not be adjusted to differentiate between purposely reduced excitation during light load periods and loss of excitation [33]. The single phase distance relay called mho relay [34] for LOF protection was first introduced in [30]. Such relay is connected at the generator terminal and looks into the generator impedance. As for all impedance elements the characteristic is being drawn on a X-R plane in which horizontal axis is resistance or real part of the impedance and vertical axis is reactance or imaginary part of the impedance. It is recommended to set the diameter of the mho relay equal to d-axis synchronous reactance X_d with the offset equal to half of transient synchronous reactance $X'_d/2$ as shown in Figure 6 [30] although other strategies are possible [20],[35],[36].

The voltage and current provided to the relay first filtered for aliasing and then by digital techniques the amplitude and phase angles were determined. These values are used to calculate different quantities such as power and impedance. The author in [30] studied the effect of different rotor constructions and system impedances on the seen impedance. The relation between loss of excitation and loss of synchronism was investigated in [37]. Using mho relay will increase the selectivity between loss of field and intentionally under excited generator [38]. As the machine begins to operate as an induction generator, the impedance seen by mho relay converges on a negative reactance value. In theory this value will be equal to the synchronous reactance at 100% slip and equal to the transient synchronous reactance at zero slip [24]. The relay performance was investigated in [20] utilizing micro machine based power system simulator including transformer and power line impedance and digital hardware required to simulate an actual relay. The author recommended a pattern classifier such as neural network to distinguish type of field fault. A comparison between conventional graphical techniques [39] and new mho relay was done in [40]. The graphical method is explained further in [41].

In [42], a phase coordinate machine model was employed whereas in [30],[22], d-q axis model was used to investigate generator transient performance under LOF. Machine performance was studied in [43] for four different modes of operations. They are under or over excited motor or generator. It is recommended in [3] to have the second circle with diameter equal to 1.0 pu for severe fault condition to trip the generator instantaneously. Generator stability under loss of excitation fault is studied in [44]-[47] and a new adaptive LOF relay using the rate of change of reactance is introduced in [48]. In [49] the effect of field discharging resistor on the generator shaft torsional torque was studied.

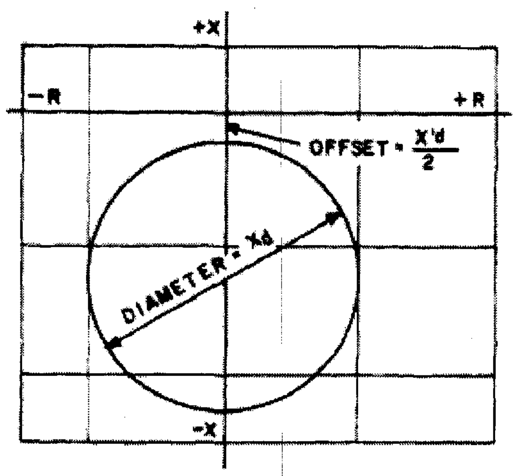

Fig. 6. Loss of excitation relay characteristic [30].

1.2 Objective

The main objective of this research work is to investigate the effect of saturation on the seen impedance by the LOF relay under loss of excitation condition. In this research work, the generator transient performance as affected by the loss of excitation conditions is studied. The IEEE3.3 dq-coordinate model of the synchronous machine has been used to predict the generator performance.

1.3 Scope

For a specific known load, frequency, real and reactive power, and terminal voltage; it is required to predict the current that will flow in the stator winding as well as the produced electromagnetic torque. The IEEE3.3 equivalent circuits have been used to develop the generator model. A computer program has been developed to solve the nonlinear differential equations in the model using a standard numerical integration technique with an iterative procedure based on Runge-Kutta algorithm.

Two different models, unsaturated and saturated, were developed and the results were compared. The terminal current and voltage phasors have been obtained and the impedance was calculated and plotted in *X-R* plane. Also the effect of load, power factor, speed control system and field discharging resistance on the transient performance were investigated in this research work.

2. Problem Definition

2.1 Loss of Excitation Transient

Electrical transient as described in [50] is an event that is undesirable but could be classified as being instantaneous, momentary, or temporarily in nature. Electrical transient is a problem for electrical power systems and could lead to misoperation of electrical equipment in the power system, overheating, tripping of the electrical machines or possible shut down. The machine transient under loss of excitation is investigated in great deals by other researchers [20]-[30]. As mentioned before under loss of excitation conditions, a synchronous generator will continue providing pulsing active power and draw large amount of reactive power from the grid which can jeopardize the system voltage stability [21]. Also the rotor of the generator will experience thermal stress due to induced eddy current because of loosing synchronism [23]. Therefore the generator can sustain internal damage and system stability can be lost [20]. Detailed study of these research works has been done to understand the transient a generator and system will experience under LOF.

As it mentioned before, LOF can be detected by an impedance mho relay [30]. The LOF relay can have two circle characteristics [3]. One with time delay and diameter equals to d axis steady state synchronous reactance and one without time delay and diameter equals to 1.0 pu. The functionality of this protective setting was investigated by other researchers with modeling the synchronous machine with different details and complications [40]-[43]. It was reported nuisance tripping of LOF relay under stable system swings [29],[39]. This was the subject of a few research works to answer this question or come up with other techniques or relay settings to prevent nuisance tripping or improve relay performance [48],[51]. In [21], a pre-modeled machine with required hardware representing actual LOF relay was studied and the author believed the conventional settings are satisfactory to protect the generator. In some cases the wrong installation of the relay or wrong wiring were blamed for nuisance tripping of the LOF relay [46]. When the LOF initiates the impedance seen by the relay starts moving from an initial point which is in the positive resistance and reactance region towards negative reactance and still positive resistance area. The shape of the seen impedance and its behavior through the journey from initial point to the entering point to the LOF relay characteristic were studied to some kind of extents by researchers neglecting machine saturation [20],[30]. The use of neural network to detect LOF fault and distinguish type of faults were recommended in [24]. In this research work, the impedance trajectory from the initial stable point all the way to the entering point to the mho circle will be investigated in great detail and the effect of initial working condition, field discharging resistance, speed control loop parameters and saturation on this trajectory will be shown. Based on the result a new relay setting will be recommended. Since the diameter of the recommended setting is smaller than the one of the conventional circle the new relay settings will reduce the chance of nuisance tripping due to stable swing and disturbance. Also the potential of utilizing of pattern recognition techniques to distinguish fault types will be discussed. As Figure 7 illustrating, filed of synchronous generator is fed by a DC source before fault occurrence or pre-fault period which is 0.1 sec. Then field being short circuit with different values of discharging resistance Figure 8.

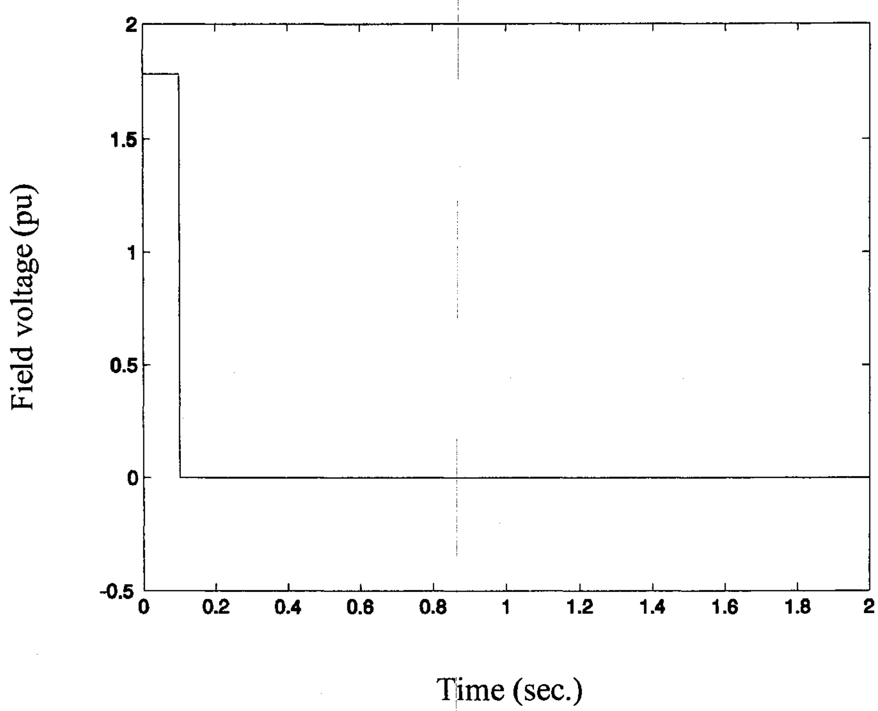

Fig. 7. Field voltage fault profile.

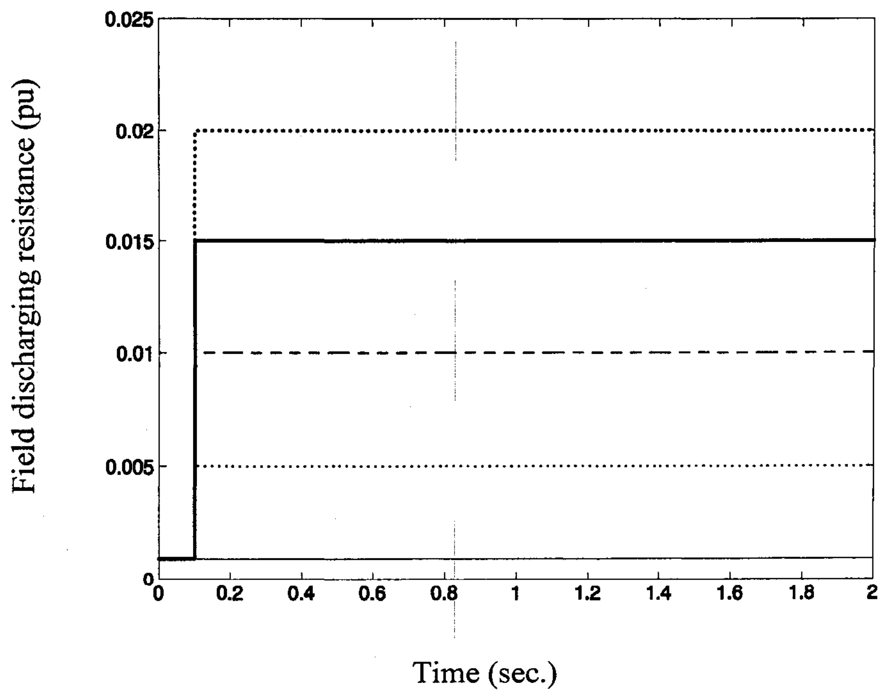

Fig. 8. Field discharging resistance fault profile.

2.2 Saturation

Even though, understanding and being able to predict the dynamic performance of synchronous machine subjected to an electrical transient is essential; the effect of saturation on electrical transients under loss of excitation condition on the machine dynamic performance has not been widely investigated. The accurate calculation of the stator, field and damper winding currents depends on the saturation conditions of their main flux [52]. Saturation is a very common phenomenon in nature. For any electrical machine, saturation of flux occurs in the ferromagnetic core. The magnetic saturation is very important in analyses of synchronous machines [53]-[56]. Analytical treatment of this nonlinear effect requires mathematical representation of the flux linkage-current relationship of the machine winding. This relationship, owing to hysteretis, is a nonlinear function [57]. Various mathematical models developed to take this nonlinear effect into account when numerical model of a synchronous machine is desired. Different researchers have proposed different methods to model saturation in synchronous machine [58]-[60]. Expressing saturating in terms of variable magnetizing inductance has been used in [61]-[63] although other techniques such as using auxiliary current source [64], [65] is available. In this research work the first method will be used. A polynomial function will be used to represent saturation characteristic obtained by the steady-state on-load measurements. Inclusion of saturation requires repeated solution of all machine equations at every time step of the simulation. Two machine models will be considered.

Model 1: saturation is ignored.

Model 2: saturation in both the direct and quadrature axes is considered.

Although the q axis saturation is considered in this research work but according to the saturation characteristic [71] and machine working condition, ignoring q axis saturation does not scarify accuracy for investigating transient performance under particular loss of excitation fault. This fact is not true for d-axis saturation. It will be shown that the d-axis saturation has noticeable effect on the transient behavior. Comparison will be made between the results calculated by the two models to show the importance of inclusion of saturation in both direct and quadrature axes for more realistic dynamic performance prediction of the synchronous generator under loss of excitation condition. Having more realistic model of synchronous generator could be used for better EMTP programs for dynamic relay testing and real time digital simulator [66],[67].

2.3 Synchronous Machine Modeling

There are several kinds of synchronous machine models with different complexity and sophistication. Modeling and simulation of synchronous machine are traditionally based on the dq-axis model. This model can provide an accurate representation of internal machine phenomena and has therefore some advantages in modeling magnetic saturation [68] and simulating machine internal faults. It can also reduce the difficulties in interfacing generator model with power system network. An alternative method that uses direct phase-domain representation is also available. The phase-domain method requires the self and mutual inductance data of various machine windings which are usually not available [69]. The widespread direct and quadrature axis model based on Park transformations has been used for machine transient performance study by many researchers. This model can be classified by the number of damper circuits in d and q axis equivalent circuits. For power system stability studies, based on experience, judgment and intuition, and often a lack of data, it has been found sufficient to limit the number of rotor circuits to a small number usually three as maximum [70]. As mentioned before rotor of a generator that lost excitation will experience induced eddy current in rotor body. Using damper circuits in d and q axis is one way to represent the path for these induced currents. The most complex (model 3.3 or order 3) has a field winding and two equivalent direct axis rotor iron windings. The quadrature axis structure of model 3.3 has three equivalent solid rotor iron circuits or windings. This model 3.3 will be used in this research work to investigate the generator transient performance under loss of excitation condition.

2.4 Speed Control System or Governor Modeling

As mentioned before because of the nature of LOF fault the generator will accelerate. Therefore the effect of speed control system or governor must be considered to obtain more accurate model. Depending on the complexity of the system, several models are available. A multi degree control systems were modeled in [22], [23]. In this research work a proportional and integral (PI) controller [64] will be used and the effect of proportional gain and integral action time on the seen impedance by LOF relay will be studied.

3. Synchronous Generator Modeling for LOF Transient Analysis

3.1 Equivalent Circuits

To investigate transient performance of a synchronous generator under LOF fault, the well known d-q axis generator model was used. The 3.3 d- and q-axis equivalent circuits of synchronous generators, recommended by the IEEE guide [70] are shown in Figure 9. Two damper windings in the direct axis and three damper windings in the quadrature axis have been considered. From these equivalent circuits, generator equations (1)-(3) can be derived.

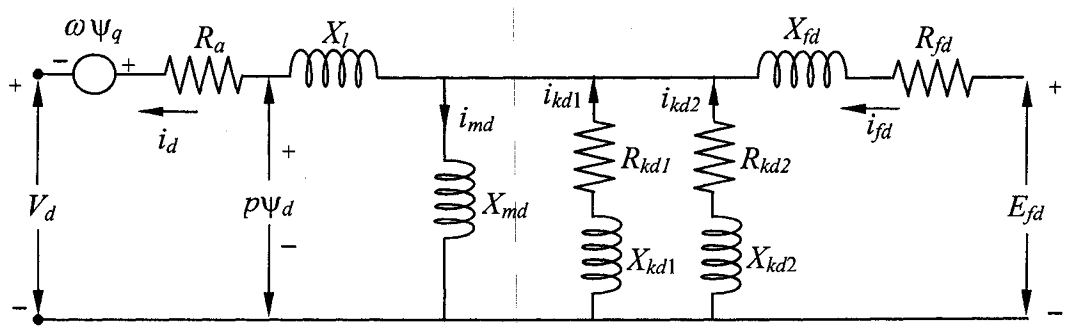

(a) d-axis

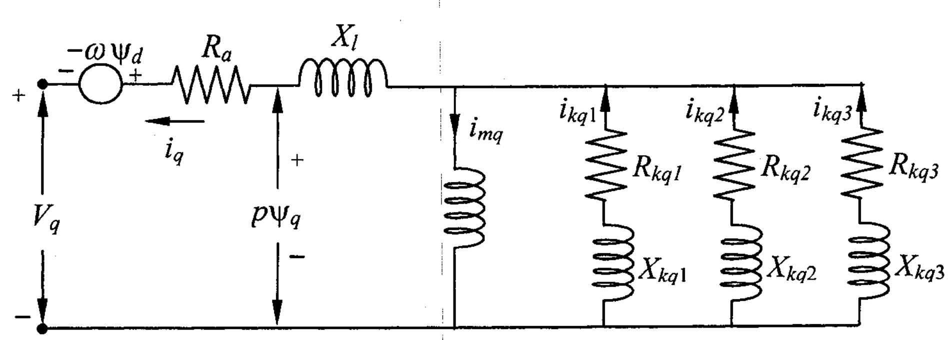

(b) q-axis

Fig. 9. d- and q-axis equivalent circuits.

3.2 Steady State Condition

To solve differential equations described in (1)-(3) the steady state operating conditions of the generator are needed. Machine phasor diagram illustrated in Figure 10 was used to calculate generator these steady-state operating conditions.

3.3 Unsaturated Machine Model

A model for unsaturated synchronous generator to investigate LOF fault has been developed using the flux differential equations.

The following assumptions in the development of the models are made:

(a) Effect of iron and stray losses are neglected.

(b) Mutual coupling effects between d- and q-axis are assumed negligible.

From the equivalent circuits of synchronous generators shown in Figure 9, stator voltage can be expressed as follows:

$$\left.\begin{aligned} p(\psi_d) &= \omega_0\left(V_d + R_a i_d + \frac{\omega}{\omega_0}\psi_q\right) \\ p(\psi_q) &= \omega_0\left(V_q + R_a i_q - \frac{\omega}{\omega_0}\psi_d\right) \end{aligned}\right\} \qquad (1)$$

Also field voltage and d-axis damper circuit voltage as follows:

$$\left.\begin{aligned} \psi(\psi_{kd1}) &= -\omega_0 R_{kd1} i_{kd1} \\ p(\psi_{kd2}) &= -\omega_0 R_{kd2} i_{kd2} \\ p(\psi_{fd}) &= \omega_0\left(V_{fd} - R_{fd} i_{fd}\right) \end{aligned}\right\} \qquad (2)$$

And q-axis damper circuit voltage as follows:

$$\left.\begin{aligned} p(\psi_{kq1}) &= -\omega_0 R_{kq1}\, i_{kq1} \\ p(\psi_{kq2}) &= -\omega_0 R_{kq2}\, i_{kq2} \\ p(\psi_{kq3}) &= -\omega_0 R_{kq3}\, i_{kq3} \end{aligned}\right\} \tag{3}$$

And according to phasor diagram illustrated in Figure 10, (4) can be written.

$$\left.\begin{aligned} & V_d = V_t \sin\delta,\ V_q = V_t \cos\delta \\ & \delta = tan^{-1}\left[\frac{I_t.X_q.\cos\theta - I_t.R_a.\sin\theta}{V_t + I_t.X_q.\sin\theta + I_t.R_a.\cos\theta}\right] \end{aligned}\right\} \tag{4}$$

Where: $\omega_0 = 2\pi f,\ f = 60\,Hz,\ p = \frac{d}{dt}$

The mechanical and developed electromagnetic torque equations can be expressed as:

$$\left.\begin{aligned} p(\delta) &= \omega - \omega_0 \\ p(\omega) &= \frac{\omega_0}{2H}\left(T - T_{em}\right) \end{aligned}\right\} \tag{5}$$

Where: $T_{em} = \psi_d\, i_q - \psi_q\, i_d$ (6)

In the determination of the transient performance due to fault at the field winding, the initial steady-state values of the machine currents and flux linkages are calculated first for a particular loading condition. To simulate the effect of the fault, the field voltage or field resistance in (2) is made equal to the fault values. This together with the initial steady-state values of the currents, flux linkages, speed and load angle at the beginning of the time step are used to find the flux linkages, speed and load angle after the fault is initiated.

The calculated flux linkages at the beginning of the step are then used to calculate the armature (stator) and damper winding (rotor) currents at the end of the step by using following synchronous machine current equations:

$$I = X^{-1}\psi \tag{7}$$

$$I = \left[i_d \; i_{kd1} \; i_{kd2} \; i_{fd} \; i_q \; i_{kq1} \; i_{kq2} \; i_{kq3}\right]^T \tag{8}$$

$$\psi = \left[\psi_d \; \psi_{kd1} \; \psi_{kd2} \; \psi_{fd} \; \psi_{kq1} \; \psi_{kq2} \; \psi_{kq3}\right]^T \tag{9}$$

$$X = \begin{bmatrix} -X_d & X_{md} & X_{md} & X_{md} & 0 & 0 & 0 & 0 \\ -X_{md} & X_{md}+X_{kd1} & X_{md} & X_{md} & 0 & 0 & 0 & 0 \\ -X_{md} & X_{md} & X_{md}+X_{kd2} & X_{md} & 0 & 0 & 0 & 0 \\ -X_{md} & X_{md} & X_{md} & X_{md}+X_{fd} & 0 & 0 & 0 & 0 \\ 0 & 0 & 0 & 0 & -X_q & X_{mq} & X_{mq} & X_{mq} \\ 0 & 0 & 0 & 0 & -X_{mq} & X_{mq}+X_{kq1} & X_{mq} & X_{mq} \\ 0 & 0 & 0 & 0 & -X_{mq} & X_{mq} & X_{mq}+X_{kq2} & X_{mq} \\ 0 & 0 & 0 & 0 & -X_{mq} & X_{mq} & X_{mq} & X_{mq}+X_{kq3} \end{bmatrix} \tag{10}$$

Where: X_d=X_{md}+X_l and X_q=X_{mq}+X_l and in this case all values are unsaturated values. The calculated currents, flux linkages, speed and load angle at the end of the step can be used to find the transient performance for the next time step.

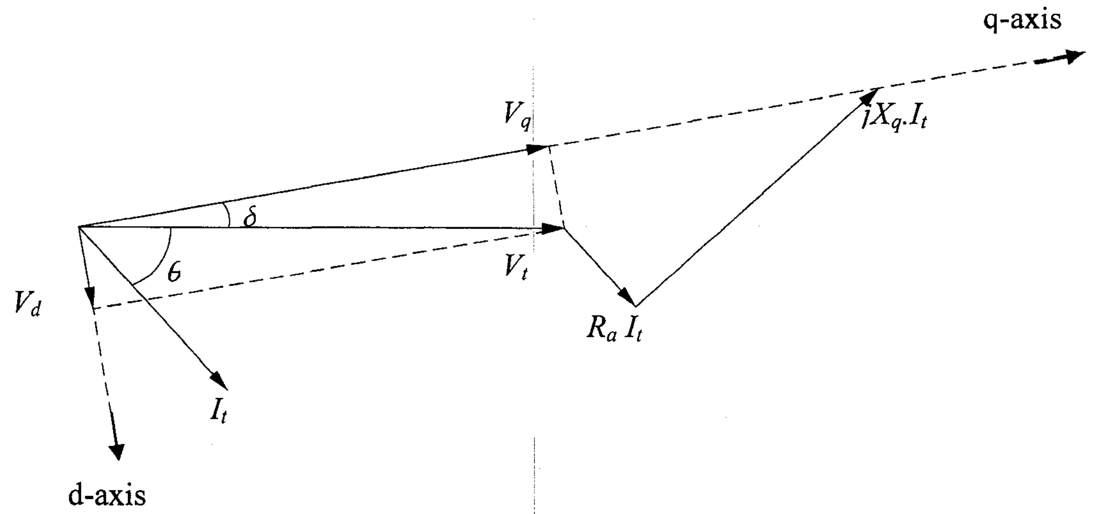

Fig. 10. Steady-state generator phasor diagram for lagging power factor.

3.4 Saturated Machine Model

Model of synchronous generator considering the saturation along the direct and quadrature axes has been obtained by modifying the unsaturated model that was described in the previous section.

3.4.1 Saturated Model considering d-Axis and q-Axis Saturation

In this case, both d- and q-axis saturation are considered. The unsaturated d- and q-axis magnetizing reactances are replaced by their corresponding saturated values. These d- and q-axis saturated magnetizing reactances, X_{mds} and X_{mqs}, are obtained by modifying the corresponding unsaturated values, X_{mdu} and X_{mqu}, with two saturation factors calculated from the polynomials fitting the saturation curves. The d- and q-axis magnetizing ampere-turns (AT_d, AT_q) are used to locate the operating points on the d- and q-axis saturation characteristics respectively.

By applying the procedure described above, the transient performance of synchronous machines considering the saturation along the direct and quadrature axes can be calculated. However, in this case, an iterative technique has to be applied to determine the transient performance as the saturated d- and q-axis magnetizing reactances are a function of magnetizing current.

3.5 Speed Control System Modeling

In order to respond to the variation in the generator electrical load and to keep the terminal voltage frequency at desired 60 Hz, a governor control system shown in Figure 11 was considered. This speed control system could be as simple as just a PI controller.

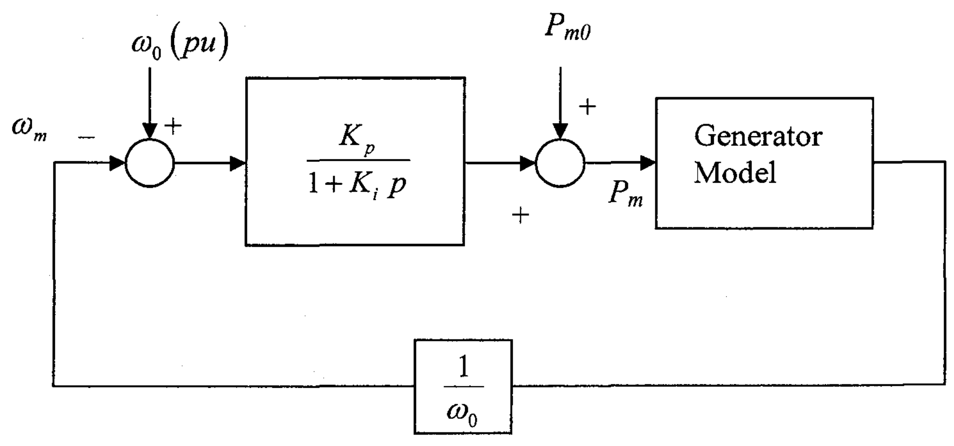

Fig. 11. Generator speed control loop

The differential equation describes the speed control loop is as follows:

$$p(P_m) = \frac{K_p}{\omega_0 K_i}(\omega_0 - \omega_m) + \frac{1}{K_i}(P_{m0} - P_m) \tag{11}$$

$$T_m = \frac{\omega_0 P_m}{\omega_m} \tag{12}$$

Equation (11) in addition to equations (1)-(5) describes the mathematical model of the synchronous generator.

4. Numerical Simulation

4.1 System Studied and Machine Parameters

The three-phase synchronous generator under investigation is connected to the infinite bus through a transmission line as shown in the one line diagram in Figure 12. The fault in the excitation system occurs at 100 ms.

4.1.1 Machine Parameters and Operating Conditions

To investigate the effect of the loss of excitation on the transient performance of saturated synchronous generators, the proposed models have been applied to a three-phase 900 MVA Hydro One Nanticoke generator [71]. The machine parameters and the initial operating conditions are presented in Table 1 and Table 2, respectively.

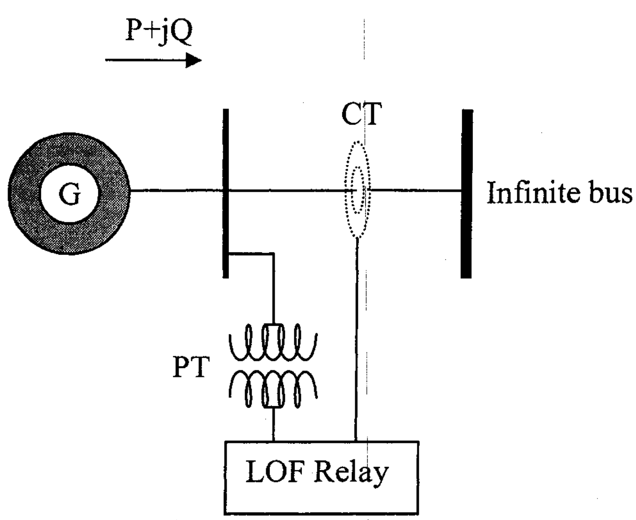

Fig. 12. Single-line diagram for the system studied.

Table 1. Machine parameters.

Rated voltage	24 KV	R_{kd1}	0.1162 PU
Rated Power	900 MVA	X_{kd2}	0.00753 PU
Frequency	60 Hz	*Rkd2*	0.00592 PU
Xmdu	2.152 PU	*Xkq1*	1.657 PU
Xmqu	2.057 PU	*Rkq1*	0.00538 PU
Xl	0.172 PU	*Xkq2*	0.1193 PU
Ra	0.0018 PU	*Rkq2*	0.1081 PU
Xfd	0.0155 PU	*Xkq3*	0.4513 PU
Rfd	0.00094 PU	*Rkq3*	0.0188 PU
Xkd1	2.732 PU	*H*	1.0 PU

Table 2: Operating conditions.

Terminal voltage	1.0 PU
Terminal apparent power	1.0 PU
Power Factor	0.866
Speed control Gain K_p	20
Speed control Integral Time T_i	2 Sec.

4.1.2 Machine Saturation Characteristics

The d- and q-axis saturation characteristics of the particular synchronous generator used in this research work are shown in Figure 13 [71]. The characteristics can be expressed by two polynomials as in (13). The magnetizing currents or ampere turns for d and q axis obtained by solving the machine equations will be used to obtain fluxes and then saturated magnetizing reactance for each axis. Then the stator and rotor currents will be calculated with respect to these new magnetizing reactances till the currents calculated in two consecutive iterations converge.

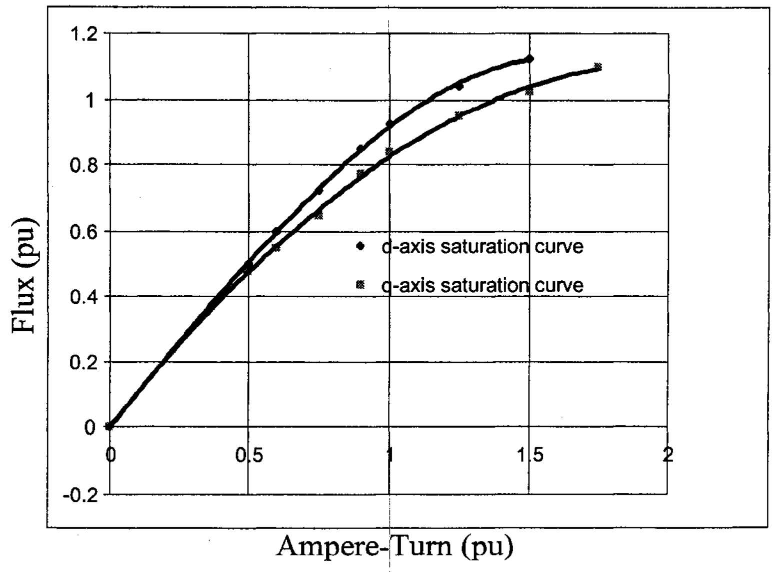

Fig. 13. d- and q-axis saturation characteristic curves [71].

$$\left.\begin{aligned}
\psi_{ds} &= f(AT_d) = -0.1501\,AT_d^3 + 0.0383\,AT_d^2 + 1.0283\,AT_d - 0.0007 \\
X_{mds} &= \frac{\psi_{ds}}{AT_d} \\
\psi_{qs} &= f(AT_q) = -0.0155\,AT_q^{\;3} - 0.2246\,AT_q^{\;2} + 1.066\,AT_q \; - 0.0012 \\
X_{mqs} &= \frac{\psi_{qs}}{AT_q}
\end{aligned}\right\} \qquad (13)$$

4.2 Simulation Flowcharts

4.2.1 Procedures of Simulation for Steady State Conditions

In this section, the basic procedures used to perform the initial value calculation and transient simulations by the proposed models are explained.

Figure 14 shows flowchart to calculate the initial values, where, terminal voltage, apparent power and power factor are given as input. Then, the load angle (δ) of the machine can be calculated. Then, the d- and q axes components of the stator voltage and current, field voltage and currents are determined.

An additional loop has been considered for taking saturation into account. By calculating the d and q axis magnetizing currents and then using the saturation characteristics in Figure 13, the saturated d- and q-axis magnetizing reactances (X_{mds} and X_{mqs}) can be obtained. These new values of the magnetizing reactance result new values of stator and rotor currents and load angle. And if all this current values are less than $\varepsilon = 10^{-6}$, the saturation condition is met for initial conditions. Then fluxes and developed electromagnetic torque can be calculated.

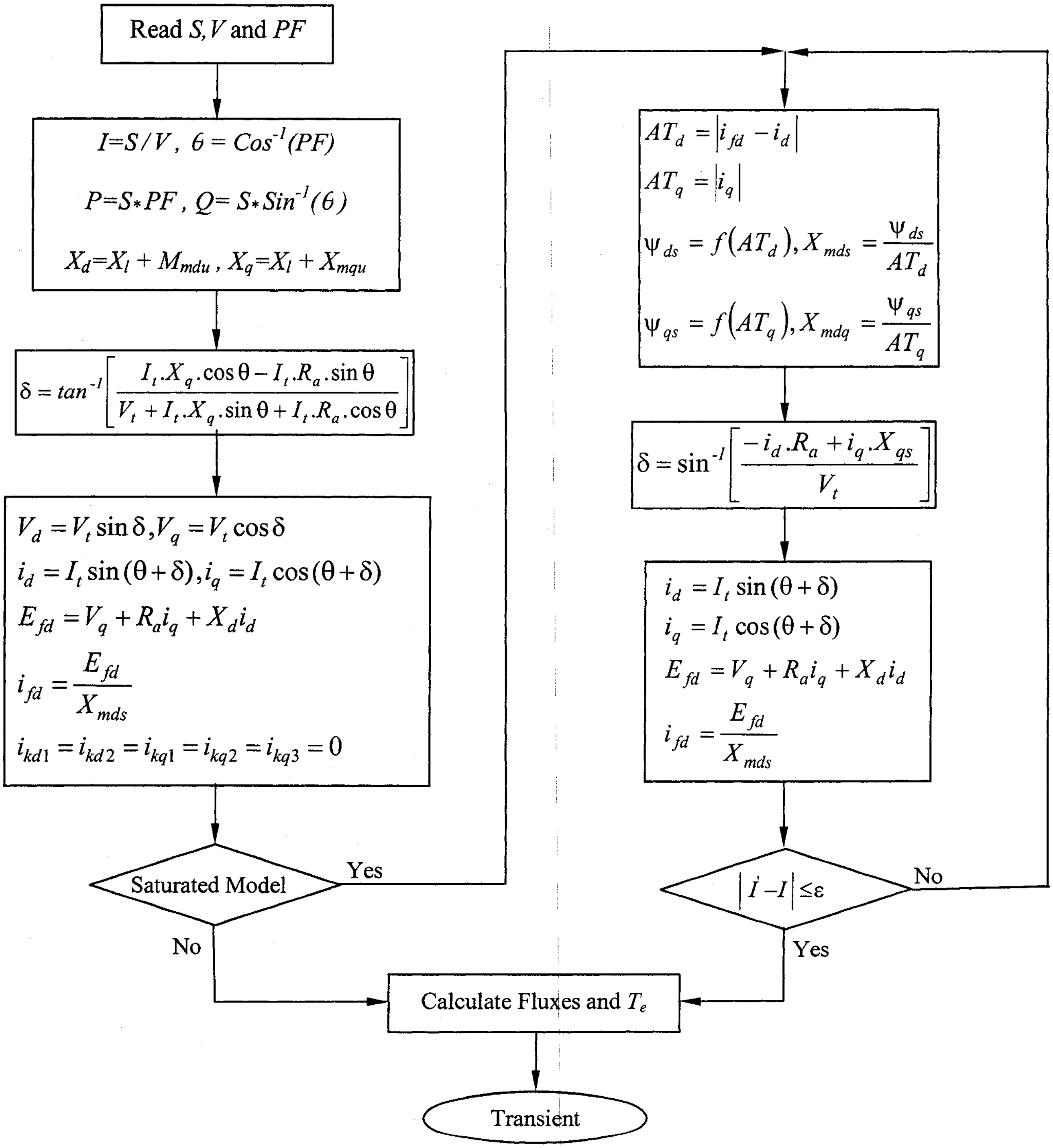

Fig. 14. Initial value calculation flowchart for saturated and unsaturated model.

4.2.2 Procedures of Simulation for LOF Transient.

To obtain transient performance of the synchronous generator under LOF fault we have to solve the system differential equations 1-3 and 11. In general, there are two methods for the integration of differential equations in power system simulation; one is an explicit method, such as the 4^{th} order Runge-Kutta method, and the other is an implicit one, such as the trapezoidal rule. In this research work explicit method has been used. 4^{th} order Runge-Kutta method was used and Figure 15 shows the flowchart.

The flowchart also illustrates an iteration process within each time step to determine saturated magnetizing reactance in both d and q axis. Basically within each time step after numerically solving differential equations and obtaining currents, saturated X_d and X_q need to be determined. This involves an iteration loop and after the currents converge then the process can proceed to the next time step.

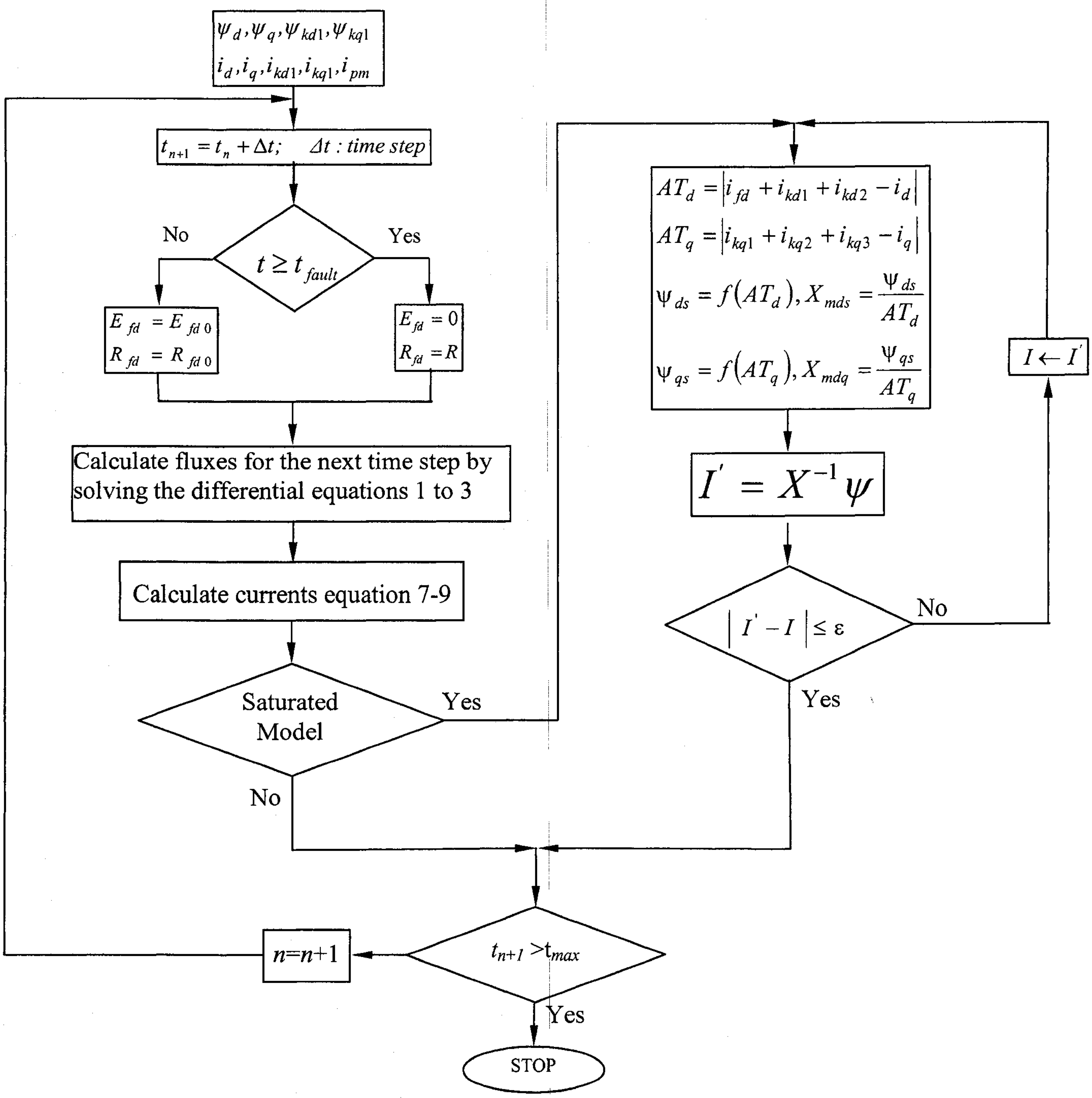

Fig. 15. Calculation of transient values after LOF fault for saturated and unsaturated model.

4.3 LOF Relay

4.3.1 LOF Relay Characteristic

As mentioned in chapter 1, LOF relay is an impedance relay connecting at the generator terminal. This relay uses generator terminal voltage and currents to calculate generator impedance. If the impedance seen by the relay falls into the relay characteristic the relay picks up and provides an alarm or trip signal after a time delay. The relay characteristic can be set and programmed with respect to generator steady state d-axis synchronous reactance X_d and d-axis transient synchronous reactance X_d'. These two values were used to draw a circle representing the relay characteristic with diameter equals to X_d and offset equals to $X_d'/2$ as shown in Figure 6.

4.3.2 Seen Impedance by the LOF relay

The voltage and current values obtained from the developed generator model were used to calculate generator impedance for different conditions and scenarios. The impedance was calculated by dividing voltage phasor by current phasor. Then the real and imaginary parts of the impedance were plotted in an *X-R* plane. The time needed for the seen impedance by the relay, can be obtained by time stamping the trajectory or run the simulation for certain period of time and see the end of trajectory point. Since time stamping will result unclear graphs the second method was chosen.

4.4 Numerical Simulation Results

In the next four sections we are going to investigate the generator transient performance under LOF for four different cases.

Case 1:

Generator performance under LOF for different values of discharging resistance will be investigated using the saturated model with speed control. In this case the fault was defined as field voltage equals to zero for different values of field resistance representing the discharging resistance. The pre-fault operating conditions of the machine are mentioned in Table 2. The fault occurs in the field circuit at time t=0.1 Sec.

Case 2:

Generator performance under LOF will be investigated for two different generator models, saturated and unsaturated models both with speed control considered. The pre-fault operating conditions of the machine are mentioned in Table 2. A short circuit occurs in the excitation circuit at time t=0.1 Sec.

Case 3:

Saturated model of the generator with speed control will be considered to investigate machine performance under LOF for different initial loading conditions. In this case, the pre-fault loading conditions of the generator will be varied to observe the machine behavior under short circuit LOF occurring at t=0.1 Sec. Three following loading conditions will be investigated.

1. Different apparent power with constant power factor.
2. Different active power with constant reactive power.

3. Different reactive power with constant active power.

Case 4:

Saturated model of the generator will be considered to investigate the generator transient behavior under short circuit LOF for different values of speed control parameters. Like the first two cases generator is working in pre-fault conditions and LOF occurs at t=0.1 Sec.

4.4.1 Case 1

Generator Performance under LOF for Different Values of Discharging Resistance

In this section the generator performance will be investigated for different values of discharging resistance. First the fault will be defined as a short circuit in the field without changing the field resistance. Secondly the fault will be defined as an open circuit or sudden insertion of large discharging resistor in the excitation circuit. Lastly the LOF impedance trajectory will be obtained for different values of discharging resistance. Figures 16 and 17 illustrate the speed and rotor angle graphs after the generator lost its excitation. The faults was defined as field short circuit or R_{fd}=0. It can be seen that somehow the generator accelerates and delta increases. Each peak or sign change in rotor angle represents a pole slip. The first pole slip occurs at about t=5 sec. and will happen again about every five seconds if the faulted generator is not cleared from the system. Figure 18 shows the generator reactive power. The pre-fault value power is positive means generator providing reactive power to the system or lagging power factor. After LOF occurs the reactive power decays and eventually the machine draws reactive power from the grid. As shown, the negative reactive power amplitude could be as large as 1.7 times rated power. This would seriously put both generator winding and system voltage stability in danger. Figure 19 illustrates the active power delivering by the generator. Although the generator still delivers power but the oscillation and amplitude could cause mechanical damage to the generator shaft and turbine. Figure 20 shows the impedance trajectory and mho relay characteristic (circle). Before fault occurs the seen impedance by the relay is in the positive resistance and reactance quadrant. After LOF fault is initiated the impedance loci is oscillatory and starts moving toward the relay circle and then enters the circle at t=2 seconds. At this time the relay will sense the fault and will provide the proper signal to trip or alarm after a preset time delay. Oscillatory behavior of the seen impedance can be explained by using Figure 9 that shows the oscillatory acceleration of the generator after loosing field. The oscillating speed will cause the same oscillating induced currants in the damper circuits (Figures 34,35) and therefore the resistance and reactance seen by the relay will oscillate accordingly (Figure 21) .

Figures 22 and 23 show the speed and rotor angle under LOF with sudden insertion of discharging resistor (R_{fd}=0.02 pu). They show a faster acceleration of the generator and, therefore, quicker approach of seen impedance toward the mho circle (Figure 26). In this case the first pole slip occurs at t=1.2 seconds and will occur again every 2.4 seconds if the generator stays online. Seen impedance will enter the circle after 0.35 second. Despite the faster behavior of the generator, by comparing Figures 24 and 25 with 16 and 17, it can be noticed that the peak values of active and reactive power are smaller in the open-circuit case. From Figure 26, it can be seen that after the fault is initiated the seen impedance moves toward the right/down side of the X-R plane and then moves back to the left/down side and the enters the circle. Figure 28 explains this behavior. It can be seen that the resistance increases first and then decreases. The sharp curve on the seen impedance can be explained by resistance as well. The change in the resistance value can be explained by the fact that before the fault occurs there is no current flowing through damper circuits therefore their resistance can not be seen by the relay. The value of this resistance depends on the value of the induced currents. Figures 29-31 show the total terminal and the largest d- and q-axis damper currents for different values of field resistance.

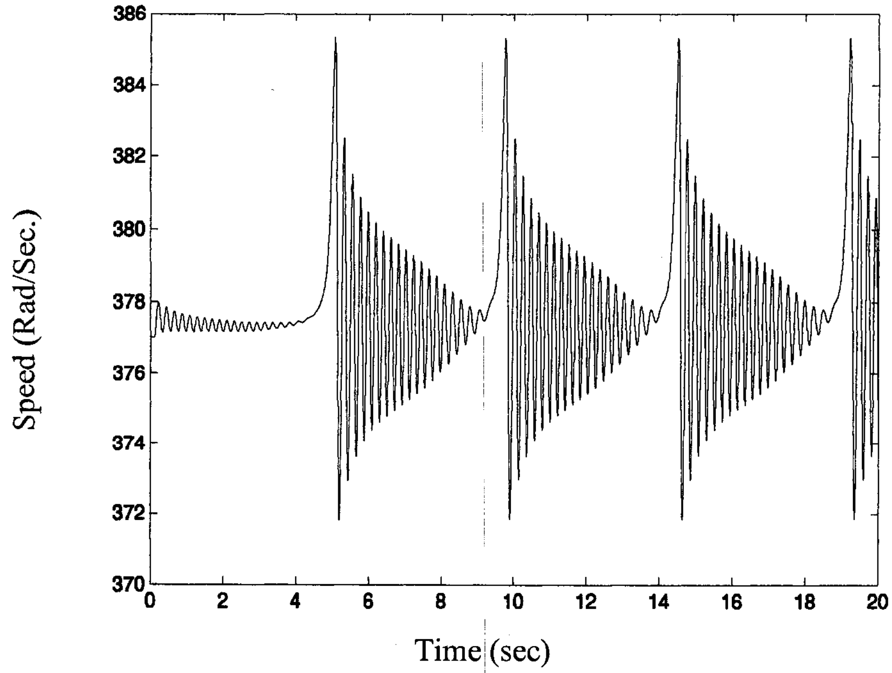

Fig. 16. Generator speed under short circuit fault in the field circuit.

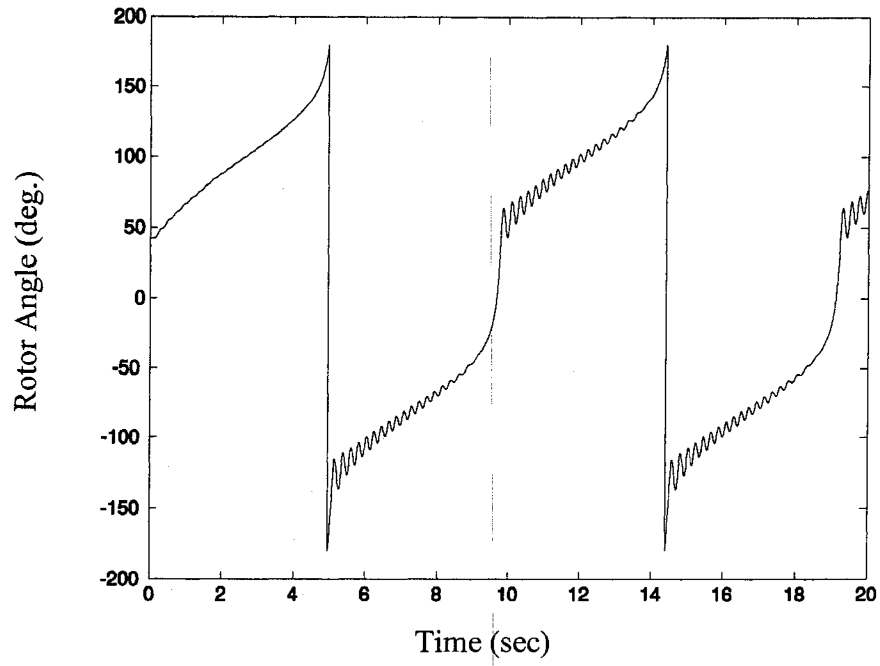

Fig. 17. Generator load angle under short circuit fault in the field circuit.

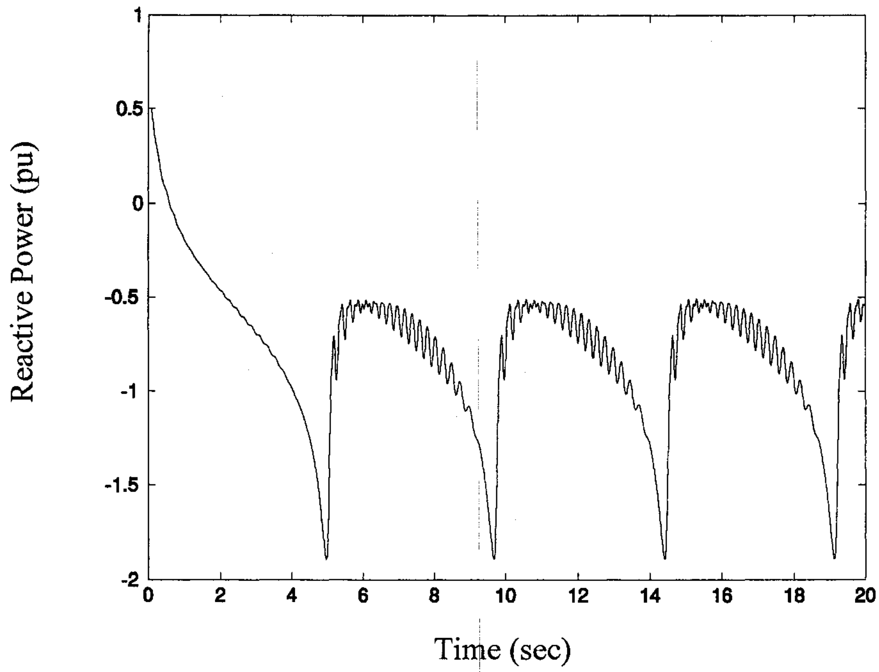

Fig. 18. Generator reactive power under short circuit fault in the field circuit.

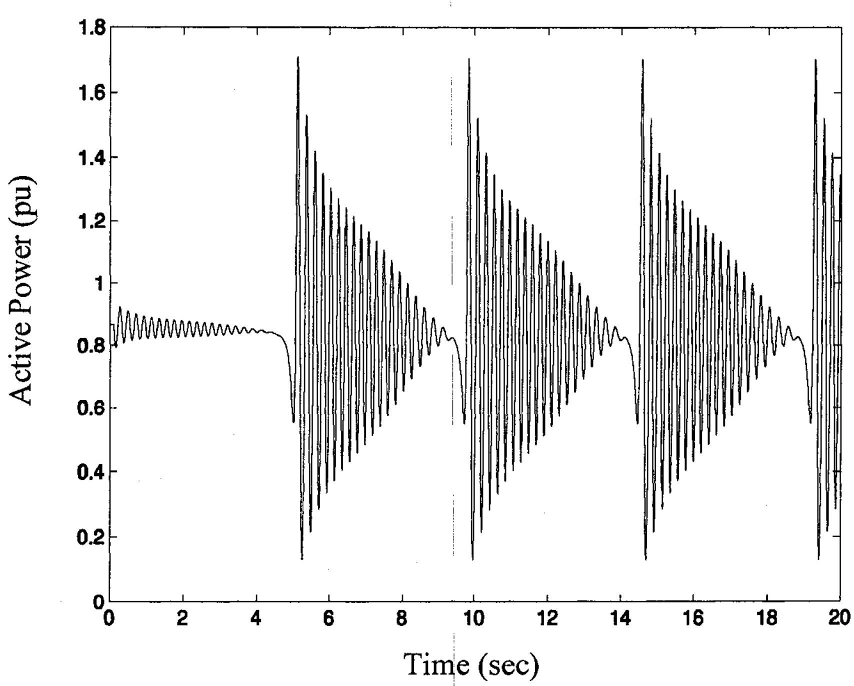

Fig. 19. Generator active power under short circuit fault in the field circuit.

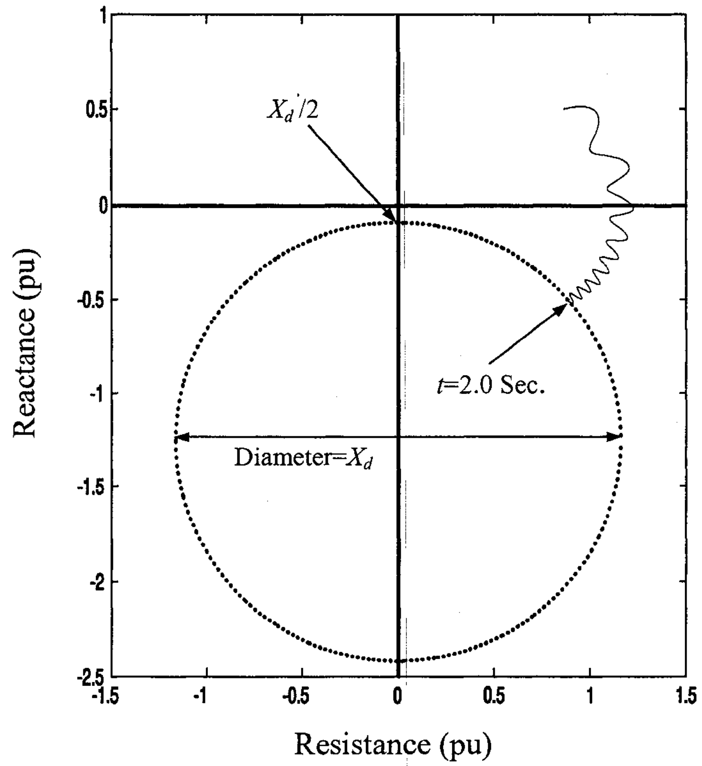

Fig. 20. Seen Impedance trajectory under short circuit fault in the field.

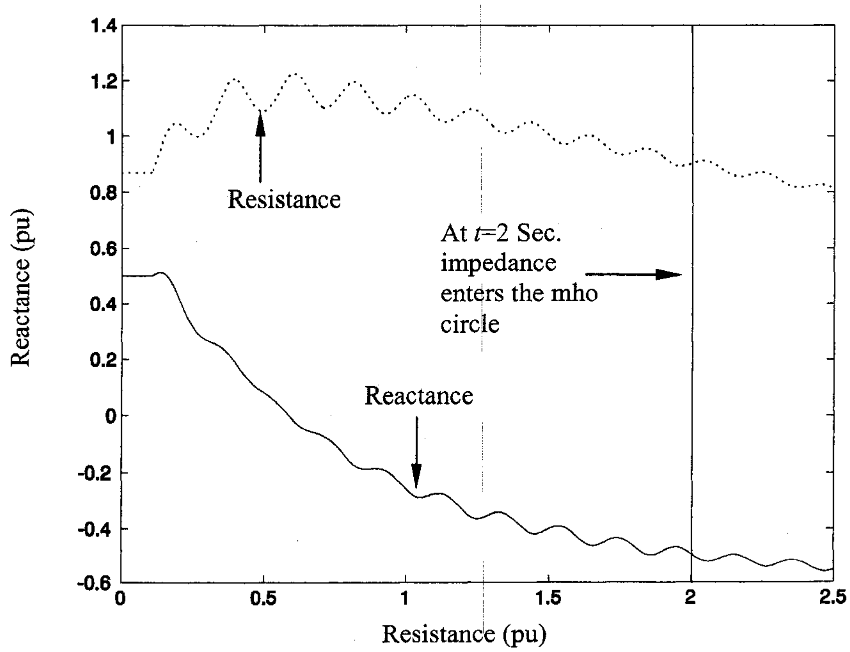

Fig. 21. Terminal resistance and reactance under short circuit fault in the field.

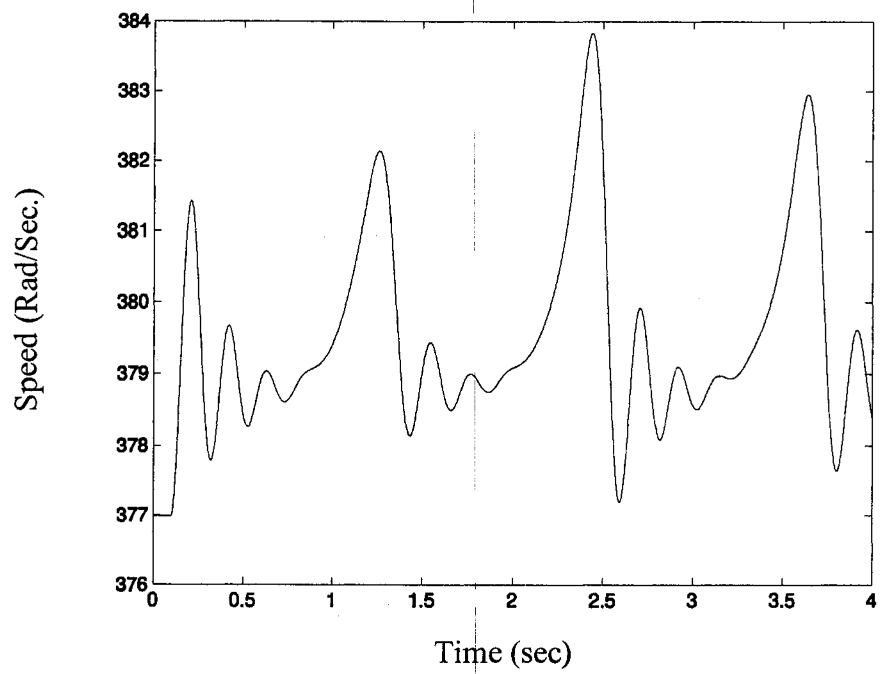

Fig. 22. Generator speed under open circuit fault in the field.

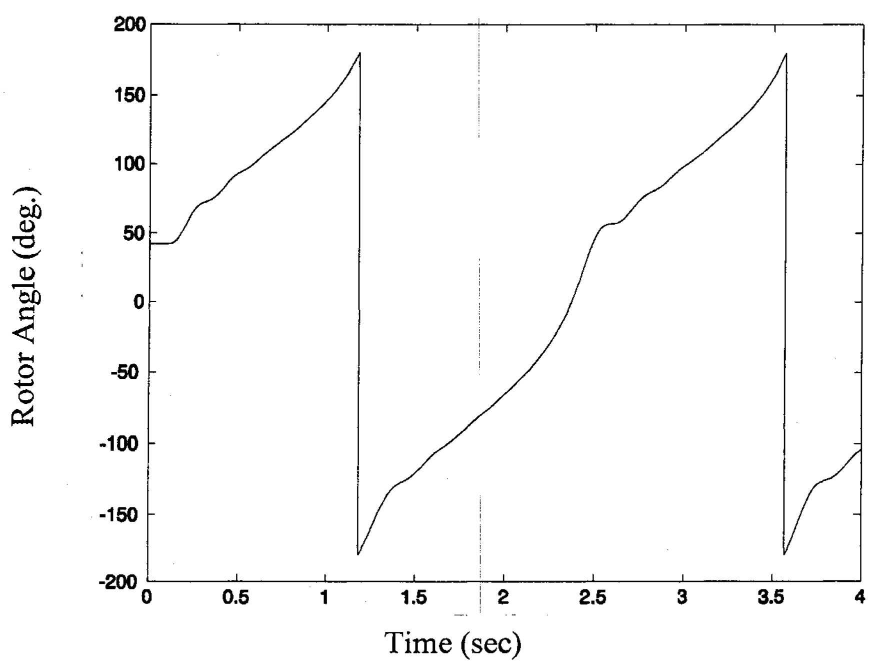

Fig. 23. Generator load angle under short circuit fault in the field.

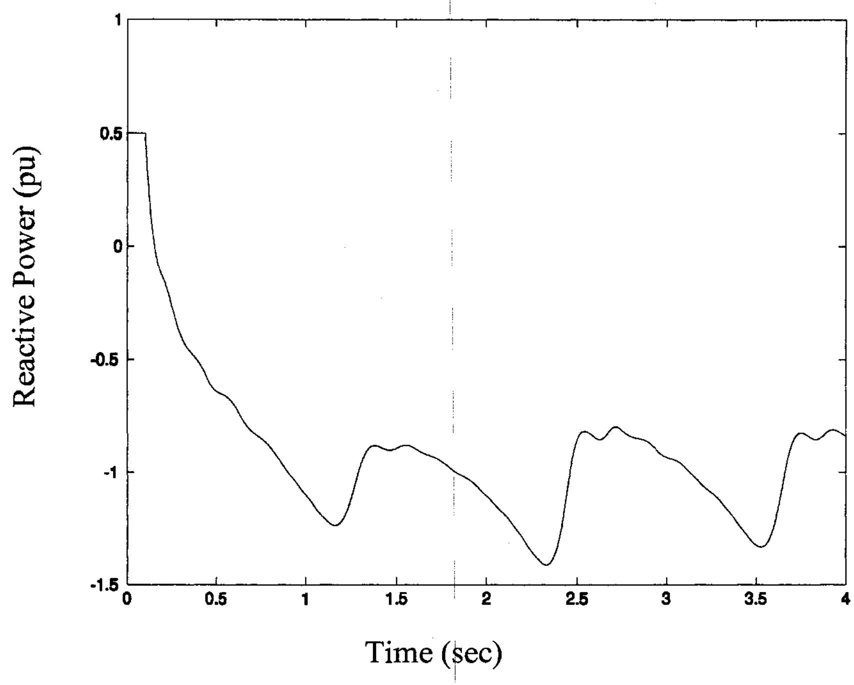

Fig. 24. Generator reactive power under short circuit fault in the field circuit.

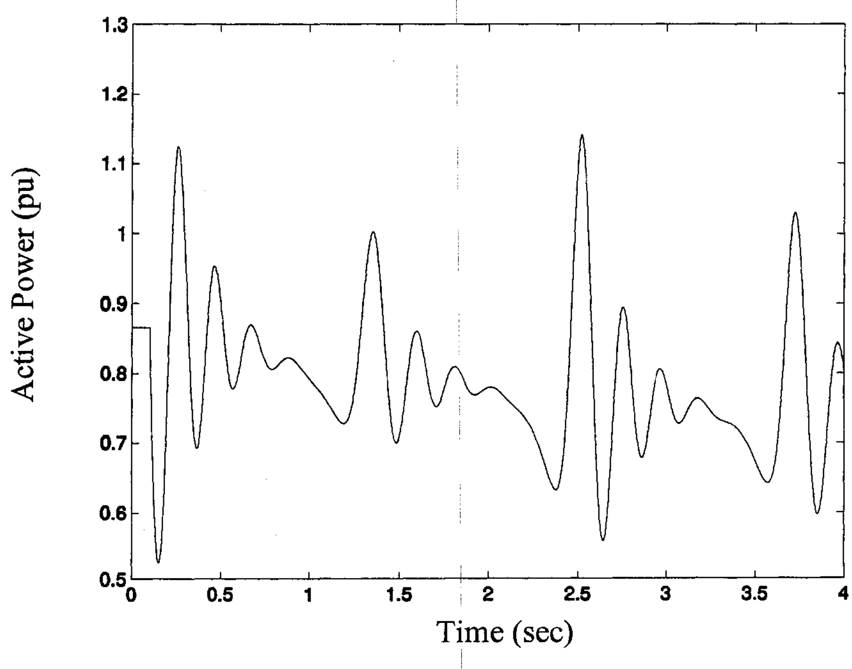

Fig.25. Generator active power under short circuit fault in the field circuit.

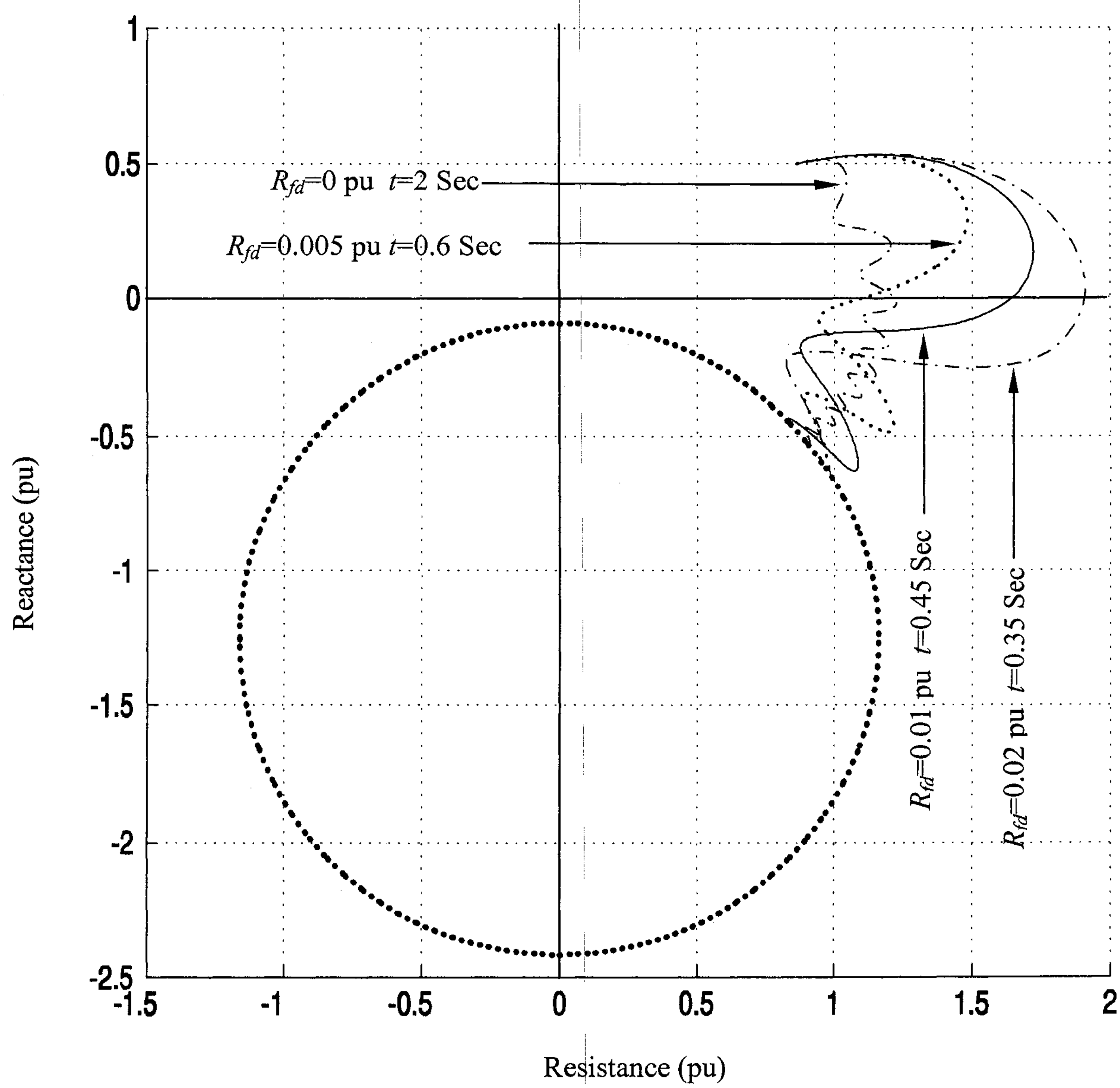

Fig. 26. Seen impedance trajectory for different values of discharging resistor.

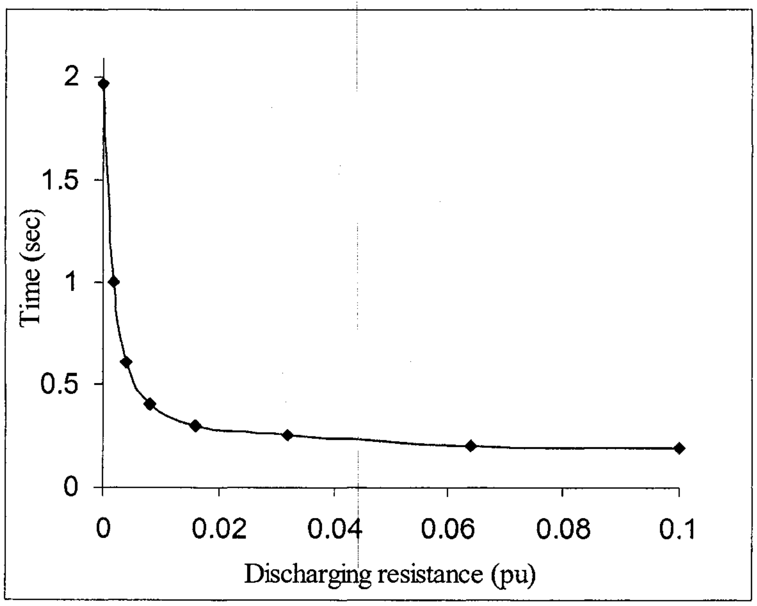

Fig. 27. Time needed for the seen impedance to enter the relay circle.

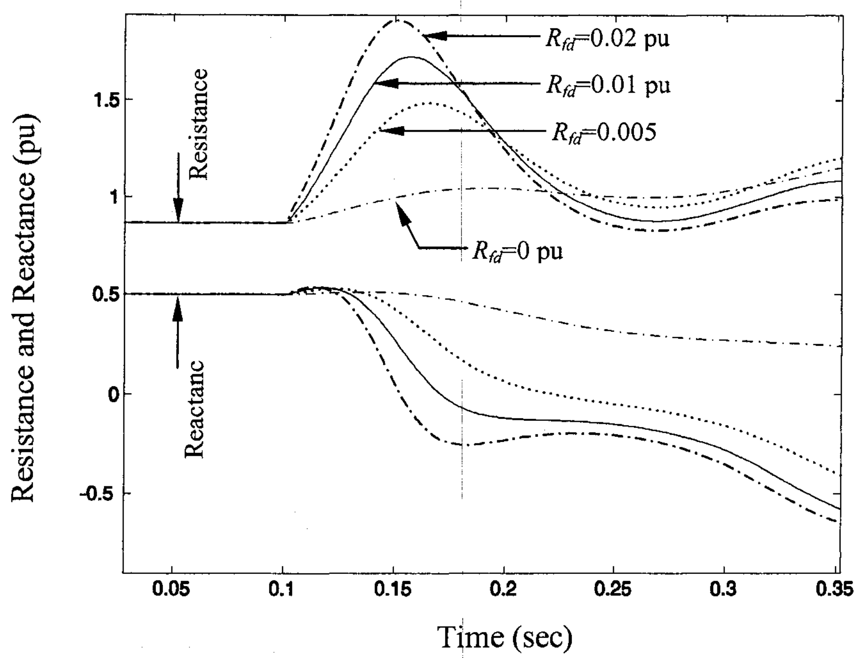

Fig. 28. Real and imaginary parts of the impedance for different values of filed resistance.

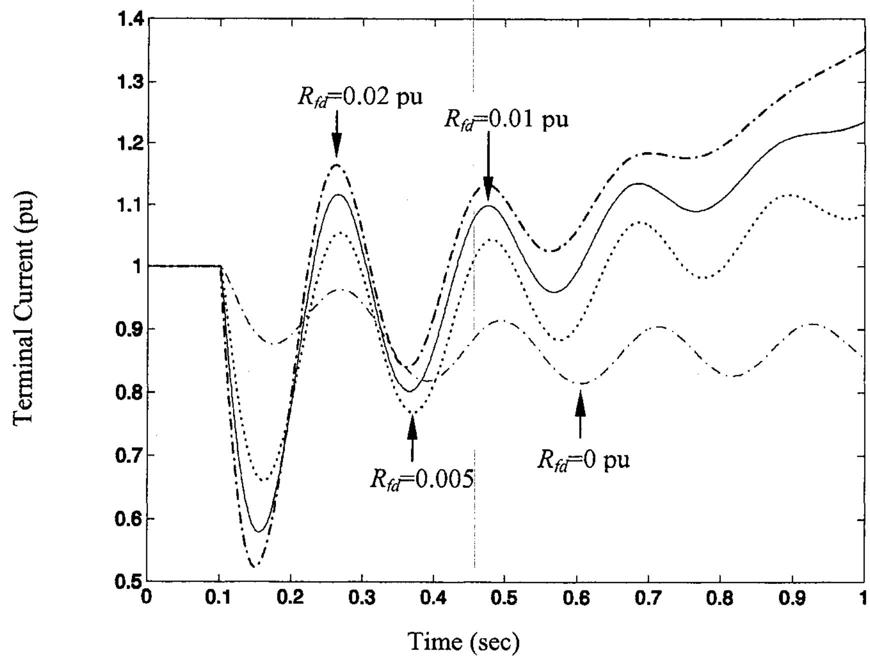

Fig. 29. Terminal currents for different values of filed resistance.

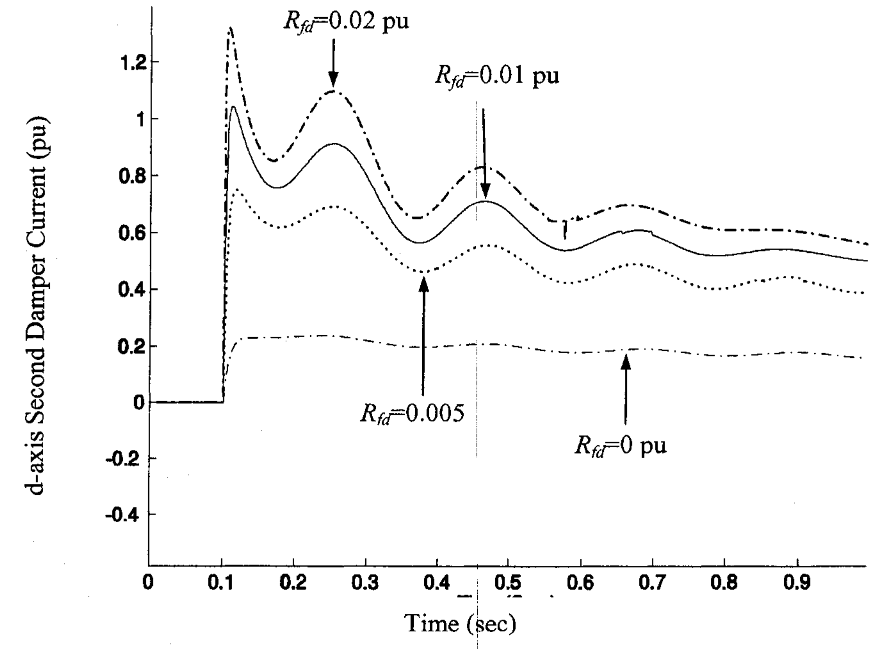

Fig. 30. I_{kd2} currents for different values of filed resistance.

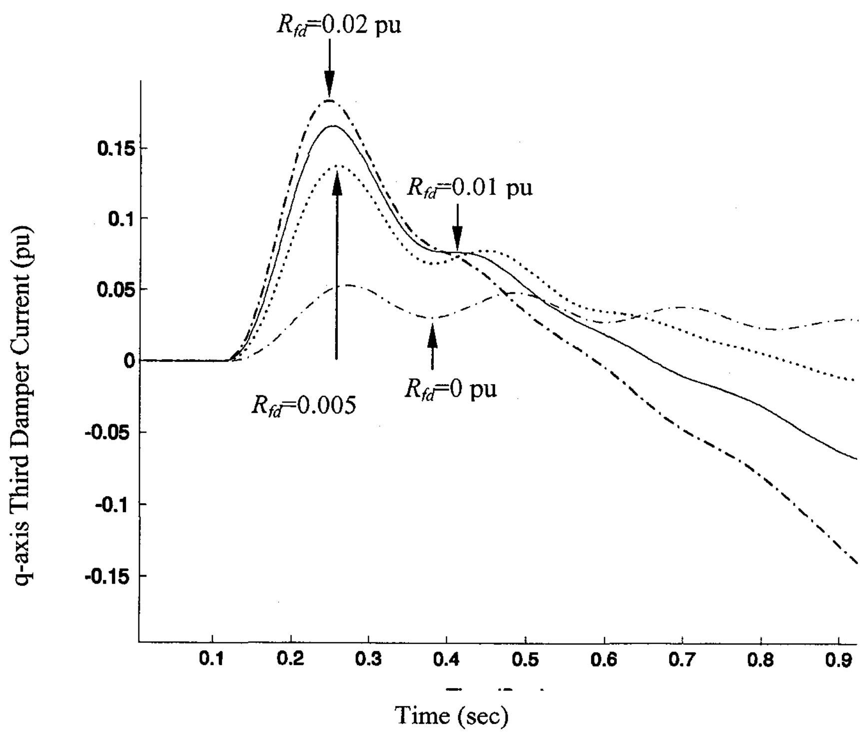

Fig. 31. I_{kq3} currents for different values of filed resistance.

4.4.2 Case 2

Effect of Saturation on Generator Transient Performance under LOF.

In this section the generator performance under short circuit in the field circuit using the two developed saturated and unsaturated models of the generator will be investigated. The generator pre-fault working conditions are the same as mentioned in Table 2. In this case, speed control system with K_p=20 and K_i=2 was considered. The short circuit in the field occurs at t=0.1 second. It can be seen from Figure 32 that pre-fault seen impedances by the relay for both models are in the same point even though the d and q axis currents are different according to Figures 35 and 36. This can be explained by the fact that the generator is working at synchronous speed and damper circuit currents are zero (Figures 35 and 36) therefore their impedance will not be seen by the relay. After the fault occurs, the impedance will be approaching the relay circle for both saturated and unsaturated models but with different speeds (Figure 32). According to Figure 33, the time for saturated model is 2.00 second and for unsaturated model is 2.53 second. The larger d and q axis current values shown in Figures 30 and 31 would explain this. This time the LOF relay will see damper circuit resistances which depend on the induced current in them. It can be noticed from Figure 34 that after fault occurs resistance or real part of the impedance increases and at about 0.7 sec starts decreasing. On the other hand, the imaginary part of the impedance or reactance is decreasing all the time. As mentioned before, the rate of change in the resistance and reactance for saturated model is greater than the unsaturated one which explains why the seen impedance enters the circuit quicker in the case of the saturated model.

As shown in Figure 38, the unsaturated impedance needs 2.53 seconds to enter the relay circle. In saturated case, if the simulation runs for the same time (2.53 seconds), the seen impedance will be at point "b" which represents the circle with diameter equal to 1.73 pu. This investigation shows that for this particular machine the relay characteristic can be set to a smaller value equal to 1.78 pu instead of X_d=2.3240 and still has the same level of protection. This can reduce the risk of nuisance trip as discussed in the second chapter.

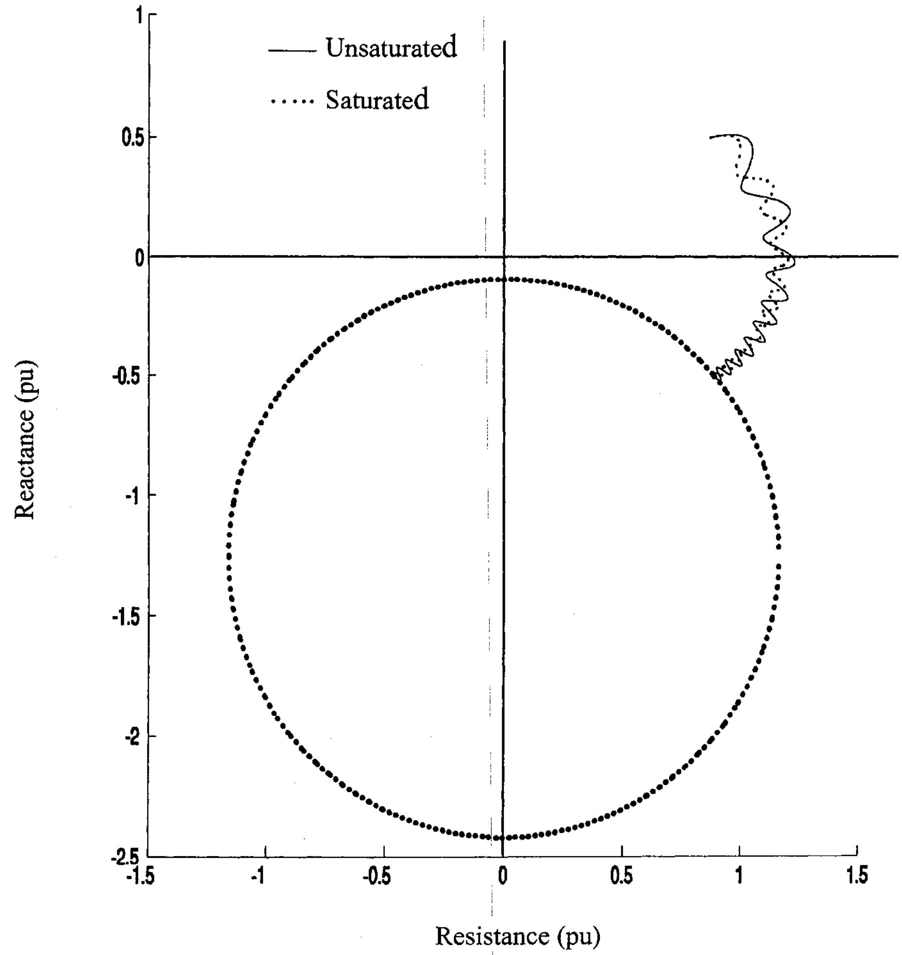

Fig. 32. Seen impedance by the relay for saturated and unsaturated model.

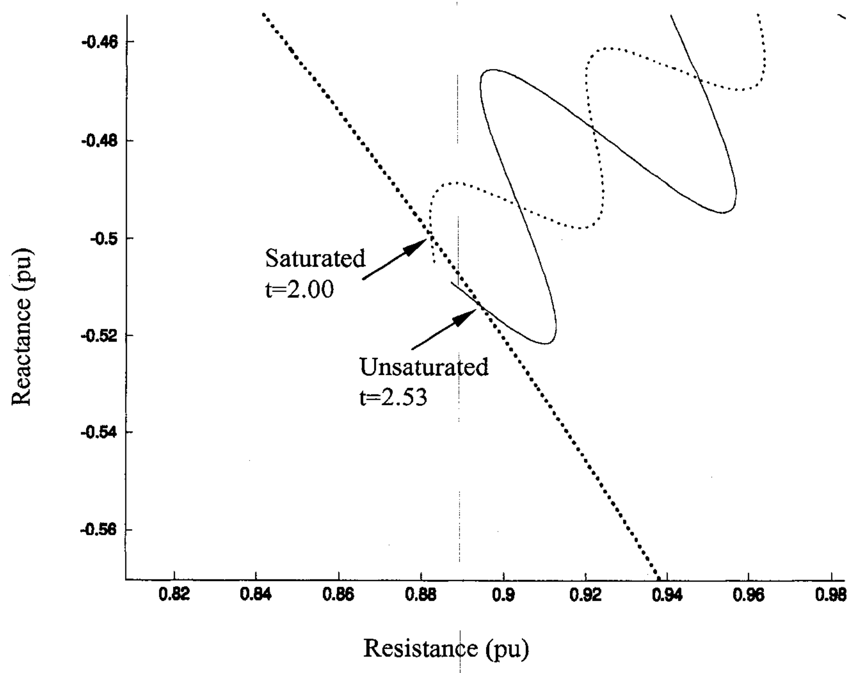

Fig. 33. Seen impedance by the relay for saturated and unsaturated model (Zoomed view).

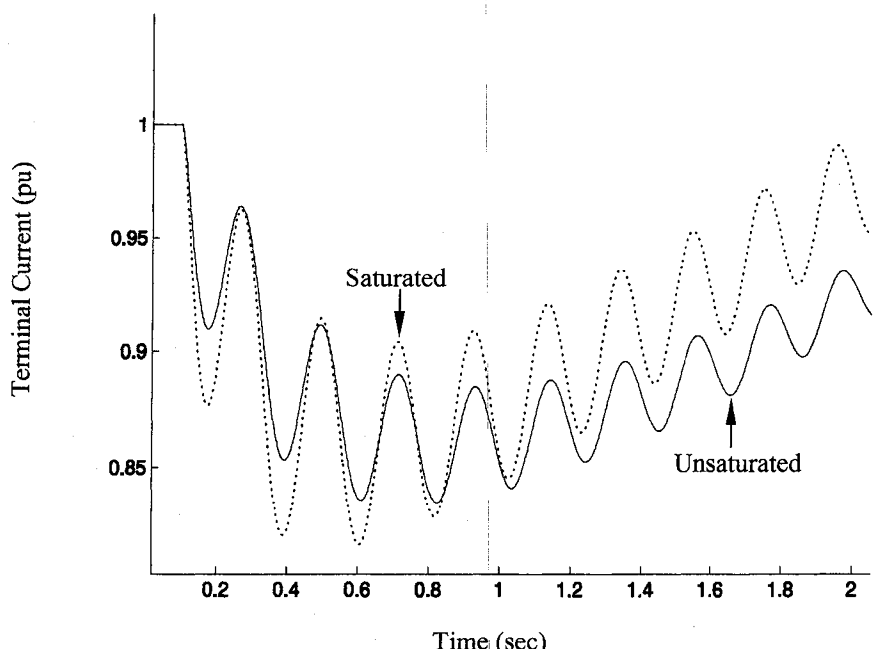

Fig. 34. Terminal currents for saturated and unsaturated model.

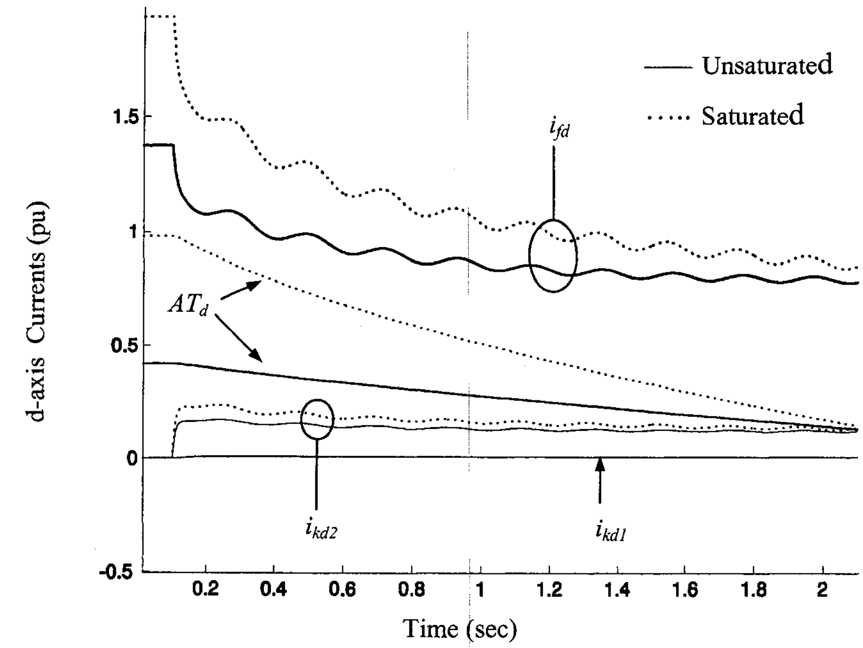

Fig.35. d-axis currents for saturated and unsaturated model.

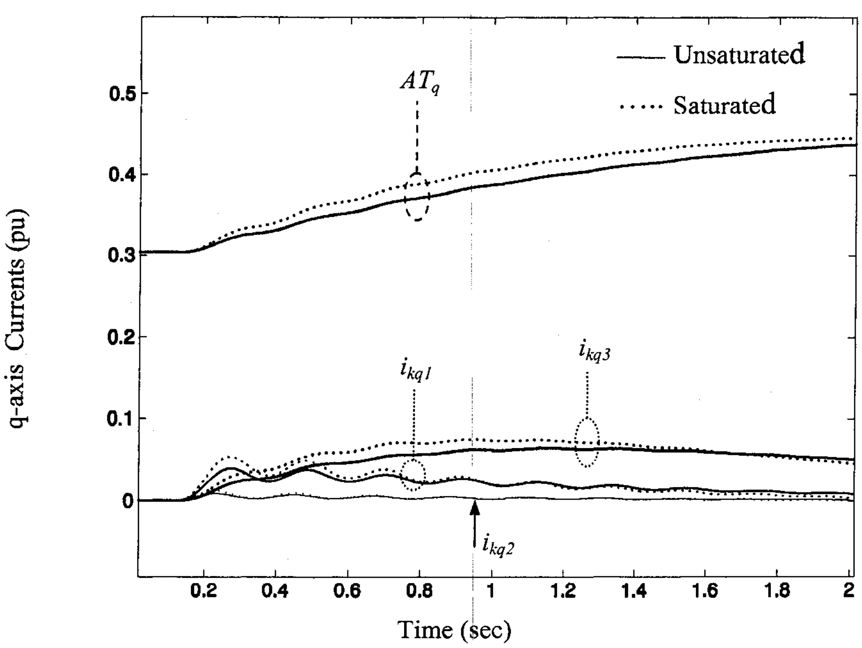

Fig. 36. q-axis currents for saturated and unsaturated model.

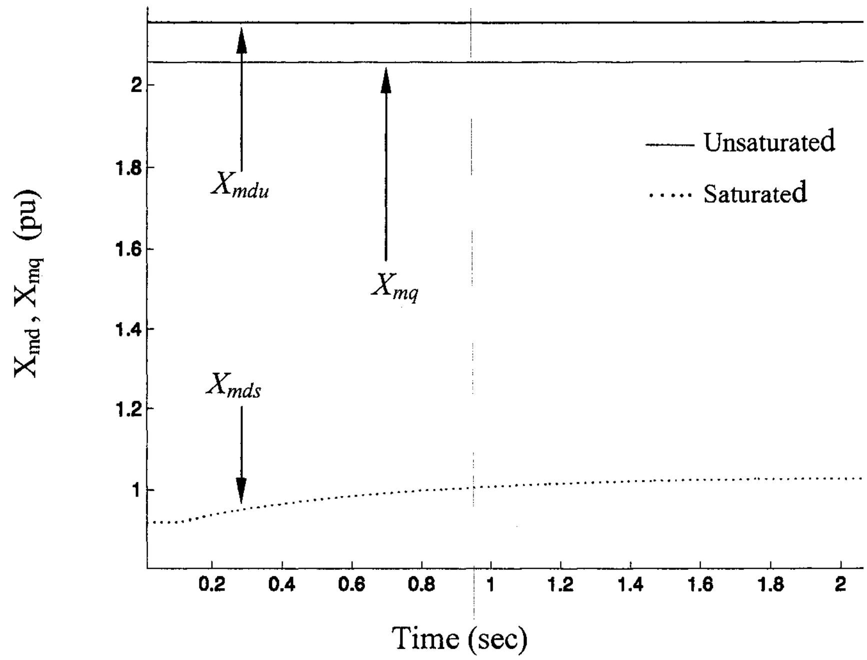

Fig. 37. d and q axis magnetizing reactance saturated and unsaturated model.

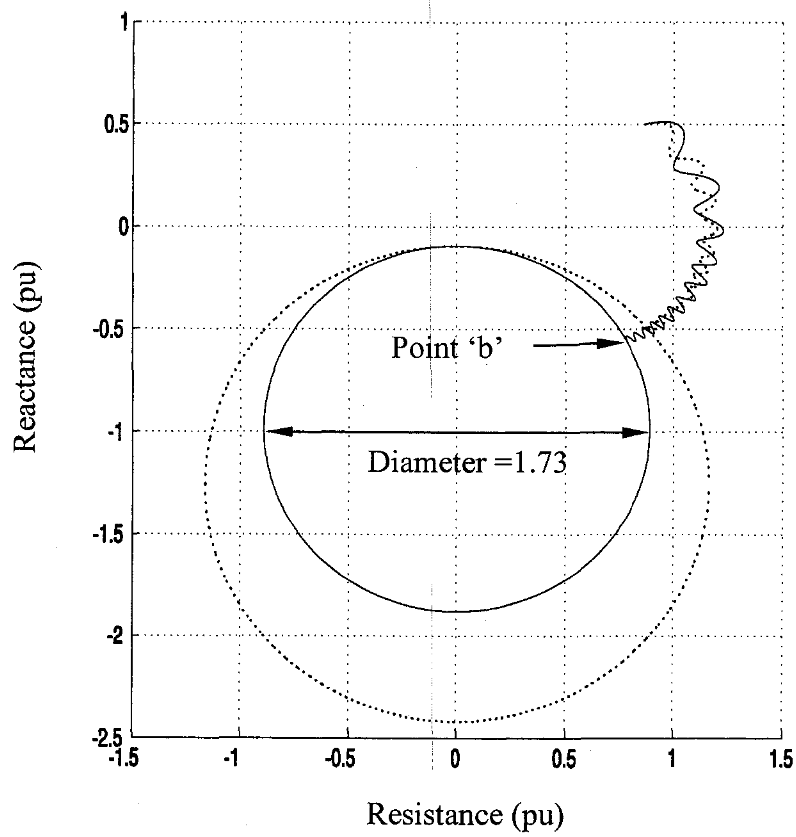

Fig. 38. d and q axis magnetizing reactance saturated and unsaturated model.

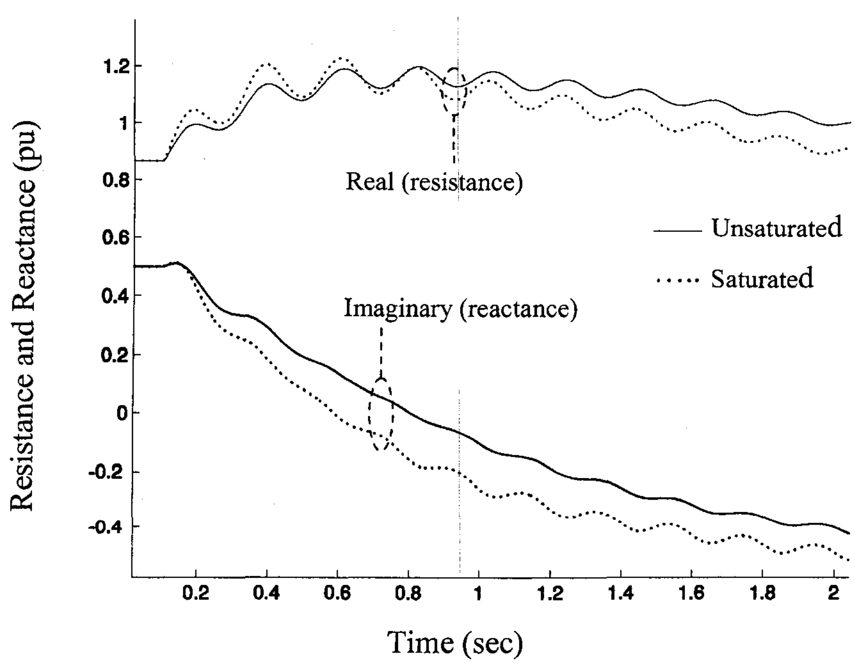

Fig. 39. Real and imaginary parts of impedance for saturated and unsaturated model.

4.4.3 Case 3

Effect of Generator Initial Conditions on Transient Performance under LOF

To investigate the effect of initial loading conditions on the generator performance under LOF, the saturated model was considered. First the initial conditions were calculated for different value of apparent, active and reactive load and then short circuit occurs in the field circuit at t=0.1 second. Figure 40 illustrates seen impedance trajectory for three different apparent powers at constant power factor. Increasing apparent power will move the initial point to down/left side of X-R plane and speed up the movement of impedance trajectory. This is because of larger slip after the excitation lost. This behavior can be explained by plotting speed, rotor angle and currents. To avoid the repetition of the same figures just the impedance will be shown. Figure 41 shows the impedance for three different active loads. It can be noticed that increasing active power moves the initial point down wards and again speed up the movement. Figure 42 shows the impedance loci for three different reactive powers. Increasing reactive power will slightly move the initial point up/left but does not have big influence on the time impedance falls inside the relay characteristic.

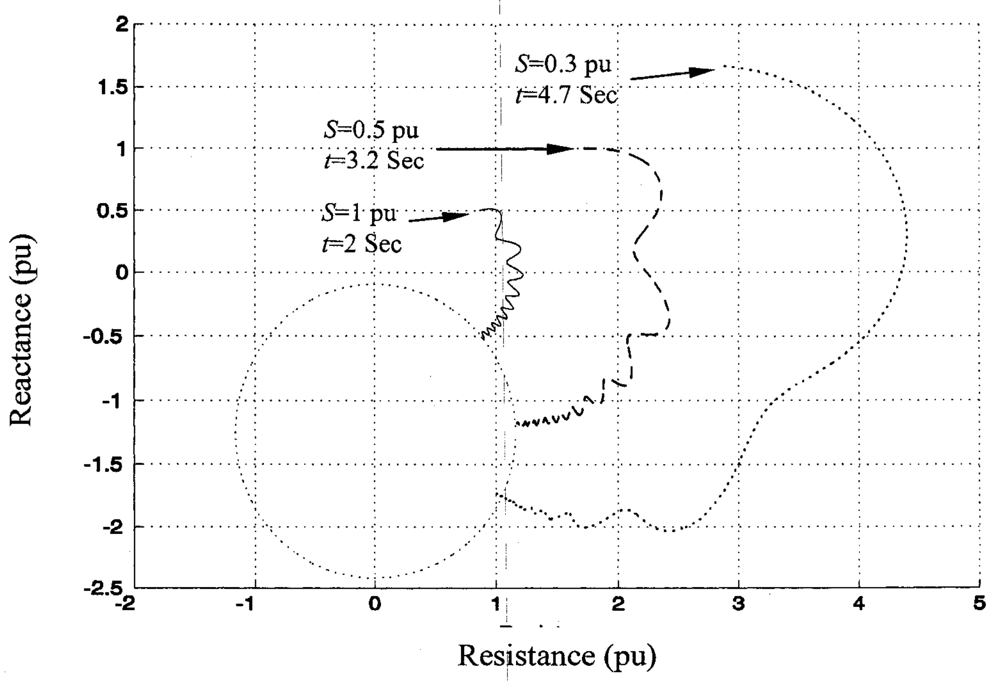

Fig. 40. Seen impedance for different apparent power conditions for constant PF.

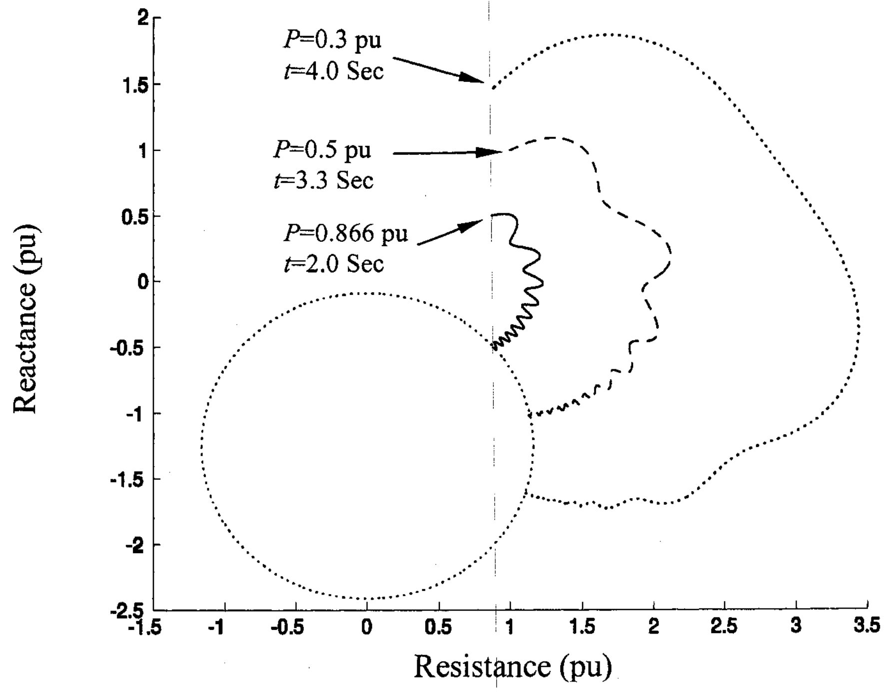

Fig. 41. Seen impedance for different active power conditions for constant reactive power.

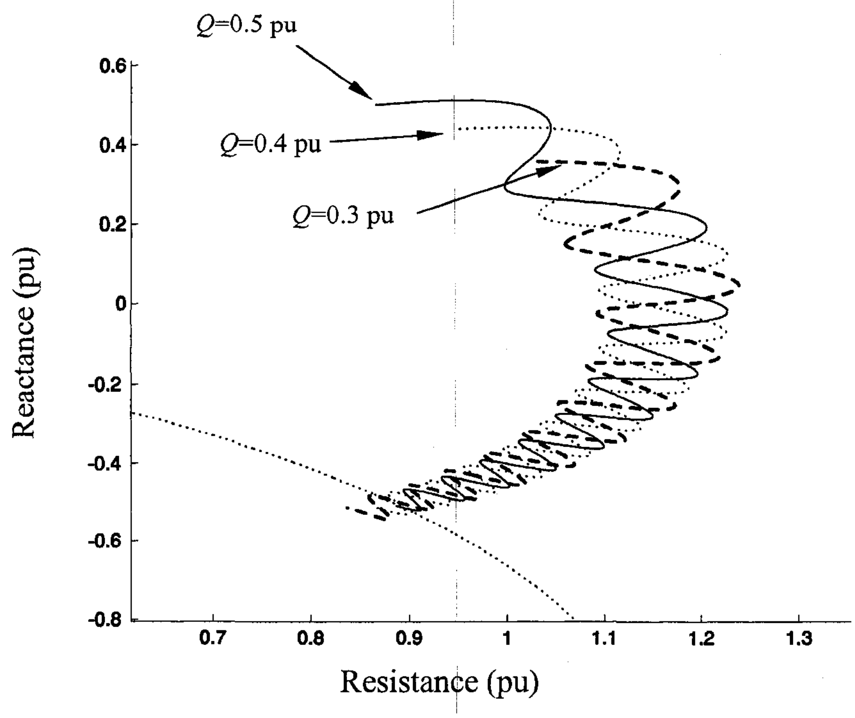

Fig. 42. Seen impedance for different reactive power conditions for constant active power.

4.4.4 Case 4

Effect of Governor System Gain and Integral Time on the Transient Performance under LOF.

To investigate the effect of control gain and integral action time on the seen impedance saturated model with load condition in table 2 was considered. Short circuit LOF occurs at t=0.1 second. In all cases simulation was run for the same time which was 2.1 seconds. For gain K_p=20 we have the same trajectory as Figure 20. It can be understood from Figure 43 that increasing controller gain will slow down impedance trajectory speed. From analysis in previous cases it was expected because speed controller will cause the governor to provide smaller mechanical power to the generator and therefore slow down generator acceleration. The Figure shows that by increasing the controller gain the impedance speed will be decreasing slightly. Figure 44 shows the effect of integral action time on the seen impedance trajectory. Decreasing integral action time will damp the speed and impedance faster but does not have a noticeable effect on the total time needed to enter the mho circle.

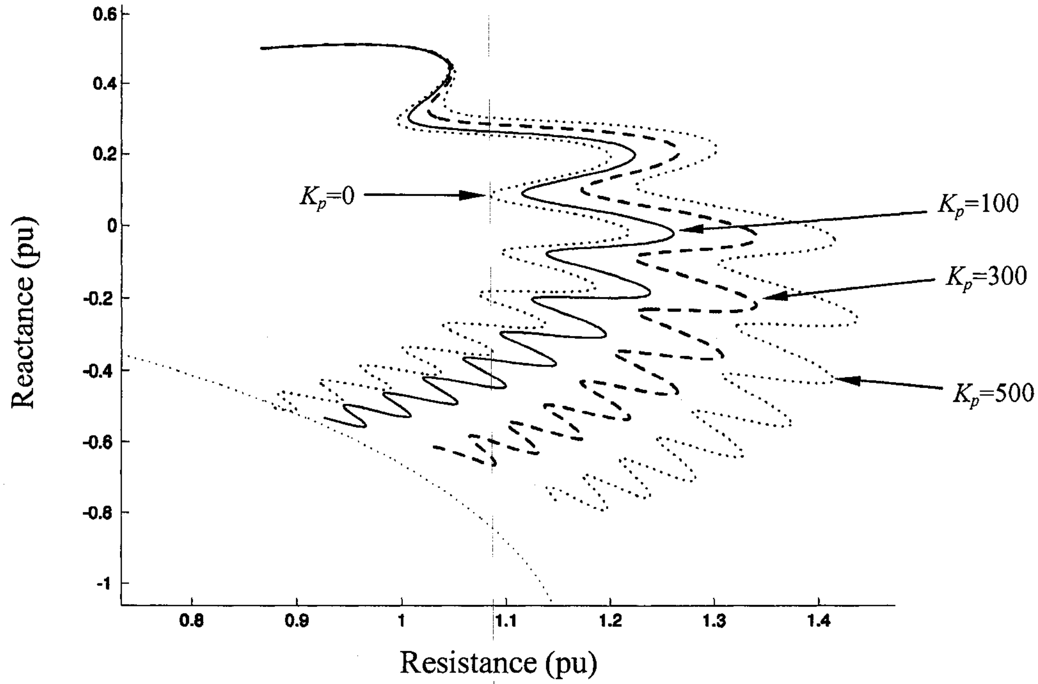

Fig. 43. Seen impedance by LOF relay under different speed control gain for K_i=2.

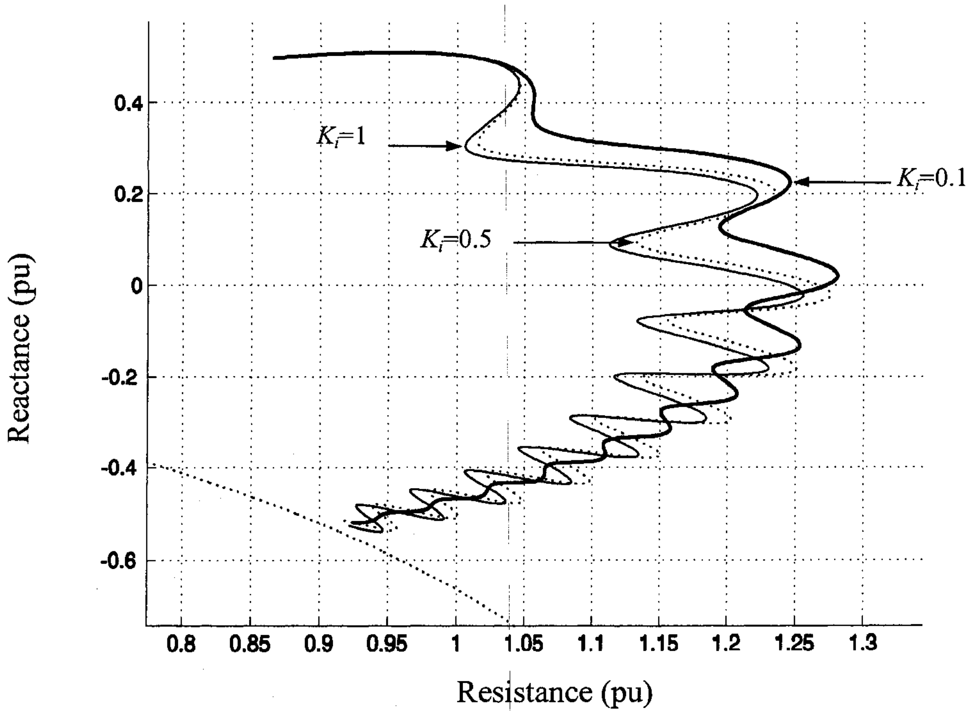

Fig. 44. Seen impedance by LOF relay under different integral time constant for K_p=20.

5. Conclusion

This research work is an attempt to develop a mathematical model for a saturated synchronous generator to investigate the effect of loss of excitation fault. In the developed model machine magnetic parameter variations due to saturation will be considered to predict the machine transient performance accurately. The following conclusions can be made from the finding of these investigations:

1. The speed of impedance approach to the LOF relay characteristic depends on the value of field discharging resistor.
2. The peak values of active and reactive power after the LOF fault is initiated depends on the value of field discharging resistor.
3. The initial point and the shape of seen impedance depend on the generator initial conditions.
4. The effect of generator initial active power load compare to reactive load is more significant.
5. There are noticeable discrepancies between the results (for example, current values and seen impedance) calculated by the models considering saturation and those calculated by the model ignoring saturation.
6. The use of the unsaturated values of the d- and q-axis magnetizing reactances can lead to significant errors in the machine transient performance predictions.
7. The effect of inclusion of d-axis saturation on the generator transient performance is significant.
8. Based on the effect of saturation on the seen impedance trajectory and its speed a new LOF characteristic is proposed.

9. Speed control gain has some effect on the seen impedance trajectory speed.
10. Although speed control integral action time has some effect on the shape and oscillation behavior of impedance trajectory but does not influence the overall speed.

References

[1] Lee D.C., Kundur P. and Brown R.D., "A high speed discriminating generator loss of excitation protection", *IEEE Trans. on Power Apparatus and Systems,* Vol. PAS-98, No.6, Nov.1979, pp. 1895-1899.

[2] ANSI Standard Device Designation Numbers. www.kilowattclassroom.com/Archive/DevNos.pdf Date: 02/15/2007

[3] *IEEE Guide for AC generator protection.* Std. C37.102.1995.

[4] *Canadian Electrical Association,* "Fundamental reliability consideration in the design, manufacturing and application of multifunction digital relays for generator protection"., April 1996

[5] GE-Multilin, "Relay selection guide", *GE power management,* General Electric Publication GET-8048A. 1998.

[6] Ranjbar, A.M., and Cory B.J., "Algorithm for distance protection", *development in power system protection, IEE Conf. Publ. 125, London,* March 1975, pp.276-283

[7] Murty V. V., Yalla S., "A digital multifunction protective relay", *IEEE Transactions on Power Delivery,* Vol. 7 No.1, January 1992.

[8] Johns A.T. and Salamn S.K., "Digital Protection for Power Systems", *British library cataloguing in publication data.*

[9] Ransick M. P., "Numeric Protective Relay Basics", *IEEE Vol. 3 on Industry application conf.,* 12-15 Oct. 1998, pp.2342 – 2347.

[10] Cheng L., Chih-Wen L. and Ching-Shan C., "Modeling and testing of a digital distance relay using Matlab/Simulink", *IEEE Power Symposium,* 23-25 Oct. 2005, pp.253 - 259

[11] Murdoch, A.; Boukarim, G.E.; Gott, B.E.; D'Antonio, M.J.; Lawson, R.A.; "Generator over excitation capability and excitation system limiters "*Power Engineering Society Winter Meeting,. IEEE Volume 1, 28* Jan.-1 Feb. 2001, pp.215 - 220.

[12] Cheng-Ting Hsu; "Under-voltage relay settings for the tie-lines tripping in an

upgrading cogeneration plant" *IEEE Region 10 Conference Vol. C, 21*-24 Nov. 2004, pp.264 - 267.

[13] *Alstom,* "Network protection and Automation" First Edition, July 2002.

[14] Kundur P., "Power system stability and control", *McGraw Hill.*, 2004.

[15] Gulez, K.; Yumurtaci, R. and Uzunoglu, M.; "The Control Of Inverse Time-Overcurrent Relay By Ann (Artificial Neural Networks) For Automation Of A System" *IEEE on Optimization of Electrical and Electronic Equipments,* Vol. 1, May 14-15, 1998, pp.241 – 244.

[16] Wu, A.; Tang Y.; Finney, D.; "MV generator low-resistance grounding and stator ground fault damage" *IEEE Transactions on Industry Application,* Vol. 40, Issue 2, March-April 2004, pp.672 – 679.

[17] Tziouvaras D.A. and Hou D. "Out of step protection fundamentals and advancements". *IEEE Conf. on protective relay engineers*, 30 Mar-1 Apr 2004, pp.282 - 307

[18] General Electric Publication, "Load Shedding, Load Restoration and Generator Protection Using Solid-state and Electromechanical Underfrequency Relays" *GET-6449,* 1974.

[19] Ito H.; Shuto, I.; Ayakawa, H.; Beaumont, P. and Okuno, K.; "Development of an improved multifunction high speed operating current differential relay for transmission line protection", *Seventh International Conference on Developments in Power System Protection (IEE,* 9-12 April 2001, pp.511 - 514

[20] Moore, P.J.; Stangenberg, A.; "An investigation into the impedance characteristics of a synchronous generator under loss of excitation condition", *International Conference on Energy Management and Power Delivery* Vo. 2, 3-5 March 1998 pp.619 – 624.

[21] Rana, R.D.; Schulz, R.P.; Heyeck, M. and Boyer, T.R., Jr.; "Generator loss of field study for AEP's Rockport plant" *IEEE on Computer Applications in Power,* Vol. 3, Issue 2, April 1990 pp.44 – 49.

[22] L. Tao; Zhou Q.; Wang X.; Su P. and Wang W.; "Dynamic performance for turbo generator under low excitation and loss of field" *Proceedings of the Fifth International Conference on Electrical Machines and Systems, ICEMS 2001.*

Vol. 1, 18-20 Aug. 2001 pp.436 – 439.

[23] Guo; K.Z.; Zhu, W.D.; Tan, F.W.; Jin, R.L. and Wang, G.; "Analysis of large turbogenerator's asynchronous operation during loss of field", *IEEE International Conference on Power System Technology*, Vol. 2, 18-21 Aug. 1998, pp.935 – 940.

[24] *GEC Alstom,* "Protective relaying application guide" T&D, 1987.

[25] Lin L.; Sun C. and Mou D.; "Study on the Excitation Protection and Control of Synchronous Generator Based on the δ and s" *IEEE on Transmission and Distribution Conference and Exhibition, Asia and Pacific* 15-18 Aug. 2005 pp.1 - 4

[26] Say M.G., "The performance and design of alternating current machines", *London, Pitman, 1948.*

[27] Agarwal P.D., "Eddy-current losses in solid and laminated iron", *AIEE Trans. on PAS,* May 1959, pp.169-181.

[28] *IEEE Tutorial on Protection of Synchronous Generators, IEEE Publication 95 TP 102.*

[29] Darron H.G.; Koepfinger J.L.; Mather J.R. and Rusche P.A.; "The influence of generator loss of excitation on bulk power system reliability" *IEEE Transactions on Power Apparatus and Systems,* Vol. 94, Issue 5, Part 1, Sept. 1975 pp.1473 – 1483.

[30] Mason C.R., "A new loss-of-excitation relay for synchronous generator", *AIEE Trans.,* Vol. 68, pp.1240-1245.

[31] E.L. Michelson and L.F. Lischer. "Generator stability at low excitation", *AIEE Trans. Vol.67, part 1, 1948, pp 1-9.*

[32] C.G. Adams and J.B. Mcclure, "Underexcited operation of turbogenerators", *AIEE, Trans. Vol.67 ,part 1, 1948, pp. 521-528.*

[33] Crossman G.C., Lindemuth H.F. and Webb R.L.. "Loss-of-field protection for generators", *AIEE Trans.,* Vol.61, May 1942, pp. 261-266.

[34] Hutchinson R.M., "The mho distance relay", *AIEE Trans.,* Vol. 65, June 1946,

pp.353-359.

[35] Dekker M., "ABB protective relaying theory and applications", New York, 1982, ABB publication.

[36] Fitzgerald A.E., Kingsley C. and Umans S.D., "Electric Machinery", *McGraw-Hill,* 1991.

[37] Elkateb M.M.; Dias M.F., "Performance analysis and design of loss-of-excitation relays. Part I" *IEEE 3rd AFRICON Conference,* Sept.22-24 1992, pp.426 – 429.

[38] Edith C., "Impedance seen by relays during power swings with and without faults", *AIEE Trans. Vol. 64,* 1945, pp. 372-384.

[39] Berdy, J.; "Loss of excitation protection for modern synchronous generators" Vol. 94, Issue 5, Part 1, Sept. 1975, pp.1457 – 1463.

[40] Warington A.R. and Van C. "Graphical method for estimating the performance of distance relay during faults and power swings", *AIEE Trans.,* Vol. 68, 1949, pp.608-621.

[41] Kimbark E., "Power system stability Vol. 2, power circuits breaker and relays". *John Wiley & Sons Inc. 6th Edition,* April 1967.

[42] P. Subramanian and O.P. Malik, "Digital simulation of a synchronous generator in direct phase quantities", *Proc. IEE.,* Vol. 118, No. 1, Jan. 1971, pp. 153-160

[43] Dias M.F. and ElKateb M.M.; "Case study into loss-of-excitation relays during simultaneous faults. II"*IEEE 3rd AFRICON Conference,* Sept. 22-24, 1992 pp.430 – 433.

[44] Clark H.K. and Feltes J.W., "Industrial and cogeneration protection problems requiring simulation" *IEEE Trans. on Industry Applications,* Vol. 25, Issue 4, July-Aug. 1989, pp.766 – 775.

[45] Ramos, A.J.P.; Lins, L.R.; Fittipaldi, E.H.D.and Monteath, L.; "Performance of under excitation limiter of synchronous machines for system critical disturbances", *IEEE Trans. on Power Systems,* Volume 12, Issue 4, Nov. 1997 pp.1702 – 1707.

[46] Arndt, C.R. and Rogers, M.; "A study of loss-of-excitation relaying and stability of a 595-MVA generator on the Detroit Edison system" *IEEE Trans. on Power Apparatus and Systems*, Volume 94, Issue 5, Part 1, Sept. 1975 pp.1449 – 1456.

[47] Rodriguez O. and Medina, A., "Stability analysis of the synchronous machine under unbalance and loss of excitation conditions" *IEEE conf. on Power Engineering Society General Meeting,* Vol. 3, July 13-17, 2003, pp.1508-1511.

[48] Tambay S.R. and Paithankar Y.G.; "A new adaptive loss of excitation relay augmented by rate of change of reactance" *IEEE Power Engineering Society General Meeting,* Vol. 2 , June 12-16, 2005, pp.1831 – 1835.

[49] El-Serafi, A.M. and Faried, S.O.; "Effect of field discharge resistors on turbine-generator shaft torsional torques" *IEEE Transactions on Energy Conversion,* Vol. 5, Issue 1, March 1990, pp.129 – 136.

[50] *IEEE Recommended Practice for Monitoring Electric Power Quality, IEEE Standards Board,* June 14, 1995, pp. 5.

[51] Hiramatsu, D.; Hirayama, K.; Tokumasu, T.; Uemura, Y. and Takabatake, M.; "Analysis of damper saturation characteristic on synchronous machine transient condition" *IEEE Power Engineering Society General Meeting,* Vol. 3, July 13-17, 2003, pp.1501-1507.

[52] Kar N.C.; El-Serafi A.M.; "Effect of the main flux saturation on the transient short-circuit performance of synchronous machines" *IEEE Canadian Conference on Electrical and Computer Engineering,* May 1-4, 2005 pp.629 – 632.

[53] El-Serafi A.M. and Abdallah A.S.; "Saturated synchronous reactances of synchronous machines" *IEEE Transactions on Energy Conversion,* Vol.7, Issue 3, Sept. 1992, pp.570 – 579.

[54] Mello F.P., "Representation of saturation in synchronous machines", *IEEE Trans. on Power Engineering Society,* Vol. PWRS-1, No. 4, 1986, pp.8.

[55] Minnich S.H., "Saturation functions for synchronous generators from finite

elements", *IEEE Trans Energy Conversion.,* Vol. EC-2, No. 4, 1978, pp.680.

[56] Boldea I., "A general equivalent circuit (GEC) of electrical machines including crosscoupling saturation and frequency effects", *IEEE Trans. on energy conversion,* Vol. EC-3, No. 3, 1988, p689.

[57] Bhadra S., "A direct method to predict instantaneous saturation curve from rms saturation curve", *IEEE Trans. on magnetics,* Vol. 18, Issue 6, November 1982, pp. 1867-1870.

[58] Levi E., "Modeling of magnetic saturation in smooth air-gap synchronous machine", *IEEE Trans. on Energy conversion,* Vol. 12, no. 2, June 1997, pp. 151-156.

[59] Ojo J.O. and Lipo T.A. "An improved model for saturated salient pole synchronous motors", *IEEE Trans. on energy conversion,* Vol. 4. No. 1, March 1989, pp. 135-142.

[60] Pekarek S.D., Walters E.A. and Kuhn B.T., "An efficient method of representing saturation in physical variable models of synchronous machines", *IEEE Trans. on energy conversion,* Vol.14, No. 1, March 1999, pp. 72-79.

[61] Schulz R.P., "Dynamic models of turbine generators derived from solid rotor equivalent circuit", *IEEE Trans. on power apparatus and systems,* Vol. PAS-92, 1973, p.926.

[62] Kundur P., "Implementation of advanced generator models into power system stability programs", *IEEE Trans. on power apparatus and systems,* Vol. PAS-102, no.7, 1983, pp.2047.

[63] EPRI, "Extended transient-midterm stability package", *EPRI EL-4610 project 1987, pp. 1208.*

[64] Tamura, J.; Takeda, I.; "A new model of saturated synchronous machines for power system transient stability simulations" *IEEE Trans. on Energy Conversion,* Vol. 10, Issue 2, June 1995, pp.218 - 224 .

[65] El-Serafi, A.M. and Abdallah, A.S.; "Effect of saturation on the steady-state stability of a synchronous machine connected to an infinite bus system" *IEEE Transactions on Energy Conversion,* Vol. 6, Issue 3, Sept. 1991, pp.514 –

521.

[66] *International Electrical Testing Association [NETA] WORLD,* Winter 2006-2007.

[67] Kezunovic M. and McKenna, M.; "Real-time digital simulator for protective relay testing" *IEEE Trans. on Computer Applications in Power,* Vol.7, Issue 3, July 1994, pp.30 – 35.

[68] Marti, J.R. and Louie, K.W.; "A phase-domain synchronous generator model including saturation effects" *IEEE Transactions on Power Systems,* Vol. 12, Issue 1, Feb. 1997, pp.222 – 229.

[69] Yu C., Dommel H.W.; Wilsun X.; "A comparative study of two synchronous Machine modeling techniques for EMTP Simulation" *IEEE Trams. On Energy Conversion,* Vol. 19, Issue 2, June 2004 pp.462 – 463.

[70] *IEEE Guide for synchronous generator modeling practices in stability analyses. Std 1110-1991.*

[71] *Ontario Hydro,* "An investigation in generator modeling for Nanticoke and Lambton generators". *Ontario Power Generation Publication.*

VITA AUCTORIS

NAME:	Hossein Tashakori
YEAR OF BIRTH:	1970
EDUCATION:	Bachelor of Science in electrical engineering Isfahan University Of Technology, IRAN 1989-1993
	Masters of Applied Science in electrical engineering University of Windsor, CANADA 2005-2007